

**Proceeding
for
International
Conference
on
Emerging Trends
in
Engineering
and
Technology
(ICET-2014)**

Published by
Technoarete Explore

Bengaluru
6th April'2014

TECHNOARETE-India



**Proceeding for International Conference
on
Emerging Trends
in
Engineering and Technology
(ICET-2014)**

Bengaluru

6th April '14

Technoarete

(A Unit of VVERT)

4A, Girija Apartment, MMDA,

Arumbakkam ,Chennai-600106,India

www.technoarete.com

Publisher: Technoarete Explore

©Copyright 2014,Technoarete-International Conference, Bengaluru

No part of this book can be reproduced in any form or by any means without prior written
Permission of the publisher.

This edition can be exported from Indian only by publisher
Technoarete Explore

Editorial:

We cordially invite you to attend the 2014 Proceeding for International Conference on Emerging Trends in Engineering and Technology (ICET-2014), which will be held in Pai Vaibhav, Bengaluru on April 6th, 2014. The main objective of ICET-2014 is to provide a platform for researchers, engineers, academicians as well as industrial professionals from all over the world to present their research results and development activities in Engineering and Technology. This conference provides opportunities for the delegates to exchange new ideas and experiences face to face, to establish business or research relations and to find global partners for future collaboration.

These proceedings collect the up-to-date, comprehensive and worldwide state-of-art knowledge on different emerging fields in Science, Engineering and Technology. All accepted papers were subjected to strict peer-reviewing by 2-4 expert referees. The papers have been selected for these proceedings because of their quality and the relevance to the conference.

The conference is supported by many universities and research institutes. Many professors played an important role in the successful holding of the conference, so we would like to take this opportunity to express our sincere gratitude and highest respects to them. They have worked very hard in reviewing papers and making valuable suggestions for the authors to improve their work. We also would like to express our gratitude to the external reviewers, for providing extra help in the review process, and to the authors for contributing their research result to the conference.

Since February 2014, the Organizing Committees have received more than 120 manuscript papers, and the papers cover all the aspects in Engineering and Technology. Finally, after review only 11 papers were included to the proceedings of ICET- 2014.

We would like to extend our appreciation to all participants in the conference for their great contribution to the success of ICET-2014. We would like to thank the keynote and individual speakers and all participating authors for their hard work and time. We also sincerely appreciate the work by the technical program committee and all reviewers, whose contributions made this conference possible. We would like to extend our thanks to all the referees for their constructive comments on all papers especially, we would like to thank to organizing committee for their hard work.

Editor-In-Chief

Dr. Nalini Chidambaram

Professor

Bharth University

Chennai

Acknowledgement

TECHNOARETE hosts the International Conference on Emerging Trends in Engineering and Technology (ICET-2014) this year in month of April. Technical advantage is the backbone of development and nano-electronics has become the platform behind all the sustainable growth. International Conference on Emerging Trends in Engineering and Technology (ICET-2014) will provide a forum for students, professional engineers, academicians, scientists engaged in research and development to convene and present their latest scholarly work and application in industries. The primary goal of the conference is to promote research and developmental activities in electronics, civil, mechanical, electrical and Instrumentation Technology and to promote scientific information interchange between researchers, developers, engineers, students, and practitioners working in and around the world. The aim of the Conference is to provide a platform to the researchers and practitioners from both academia as well as industry to meet and share cutting-edge development in these fields.

Dr. Joy Gopal Jena

HOD Dept. of Civil Engineering
SOA University
President
International Conference
Technoarete

CONTENTS

S.NO	TITLES AND AUTHORS	PAGE NO
1.	Mathematical Modeling Approach for Flood Management ➤ <i>P.Lakshmi Sruthi, P.Raja Sekhar, G.Shiva Kumar</i>	1-5
2.	Study on GIS Simulated Water Quality Model ➤ <i>P.Lakshmi Sruthi, P.Raja Sekhar, G.Shiva Kumar</i>	6-11
3.	Learning Experience in the Use of Unity: Game Engine for Development of 3D Expo ➤ <i>Tejal P. Rane, Ashvini Madival, Ningappa Arakeri, Uttam Gouranna, Priya Athani</i> ➤ <i>Priyadarshini D. Kalwad</i>	12-14
4.	Automatic Accident Detection With Traffic Light System ➤ <i>Atul Kumar, Adeesh Sharma, Girraj Sharma, Amar Singh Rajak</i>	15-17
5.	A Design and Simulation of Optical Pressure Sensor based on photonic crystal in Sub-Micron Range ➤ <i>Rajeshwari S, Indira Bahaddur, Dr. Preeta Sharan, Dr. P.C. Srikanth</i>	18-21
6.	MEMS Based Optical Sensor for Salinity Measurement ➤ <i>Shruthimala N S, Indira Bahaddur, Dr. Preeta Sharan, Dr. P C Srikanth</i>	22-24
7.	Effective Code Coverage Test Suite Generation for Java Code ➤ <i>S.Narayanan, T.Nandhinie</i>	25-28
8.	Pattern Recognition Using Video Surveillance for Wildlife Applications ➤ <i>Meghana Badrinath N, Nikhil Bharat, Madhumathi S, Kariyappa B.S.</i>	29-33
9.	Development of an EPGA-Based SPWM Generator for High Switching Frequency DC/DC Buck-Boost Converters ➤ <i>S.L.Binu, Mr.M.Afsar ali</i>	34-38
10.	Study on Internal Curing of Concrete Using Admixtures ➤ <i>A.Sivaranjani, M.Monica, V.R.Subhashini, S.Sareetha, M.S.Kuttimarks,</i> ➤ <i>Er.B.Sudhakar Senthil Vasan</i>	39-41
11.	Modeling and simulation of Solar PV Cell with MATLAB/Simulink and its Experimental Verification ➤ <i>K.Mohan, Mr.R.Dhinakaran</i>	42-47

ORGANIZATION COMMITTEE

MANAGING DIRECTOR

Asst.Prof(Sr.G) J.Selvakumar
Department of ECE
SRM University

PRESIDENT:

Prof J.G.Jena.

PROGRAM CHAIRS

Dr. Nalini Chidambaram

ORGANIZING SECRETARY

Er. Rajesh Babu
Er. A. Siddharth

PUBLICATIONS COMMITTEE

Dr. Shankar Narayanan
Dr.S. Sangeetha

Mathematical Modeling Approach for Flood Management

^[1]P.Lakshmi Sruthi, ^[2]P.Raja Sekhar, ^[3]G.Shiva Kumar

^[1]P.G.Student, ^[2]Associate Professor, ^[3]U.G.Student

^[1]kanchu1991@gmail.com, ^[2]sekharpr@yahoo.com, ^[3]shivakumar00740@gmail.com

Abstract— “Establishing a viable flood forecasting and warning system for communities at risk requires the combination of data, forecast tools, and trained forecasters. A flood-forecast system must provide sufficient lead time for communities to respond. Increasing lead time increases the potential to lower the level of damages and loss of life. Forecasts must be sufficiently accurate to promote confidence so that communities will respond when warned.

Hydrological methods use the principle of continuity and a relationship between discharge and the temporary storage of excess volumes of water during the flood period. Hydraulic methods of routing involve the numerical solutions of the convective diffusion equations, the one dimensional Saint Venant equations of gradually varied unsteady flow in open channels.

In present research, the examination of the several hydraulic, hydrologic methods, have been preceded for Godavari river data i.e., from Perur to Badrachalam stretch, compared with MIKE 11 software analysis. MIKE 11 is a professional engineering software tool for the simulation of hydrology, hydraulics, water quality and sediment transport in estuaries, rivers, irrigation systems and other inland waters. The model is calibrated and verified with the field records of several typhoon flood events. There is a reasonable good agreement between measured and computed river stages. The results reveal that the present model can provide accurate river stage for flood forecasting for the particular stretch in the Godavari River.

Index Terms—Hydrological Method, Mike 11, Software analysis.

I. INTRODUCTION

Flood is the worst weather-related hazard, causing loss of life and excessive damage to property. If flood can be forecast in advance then suitable warning and preparation can be taken to mitigate the damages and loss of life. For this purpose, many river basins have worked to build up the flood forecasting system for flood mitigations. A flood forecasting system may include all or some parts of the following three basic elements: (i) a rainfall forecasting model, (ii) a rainfall-runoff forecasting model, (iii) a flood routing model. The ability to provide reliable forecast of river stages for a short period following the storm is of great importance in planning proper actions during flood event. This article focuses on the development of the flood forecasting model.

In general, the flood routing can be classified into two categories including hydrologic method and hydraulic method. Among the hydraulic method can be widely applied to some special problems that hydrologic techniques cannot overcome and achieve the desired degree of accuracy. But, many researchers used various adaptive techniques and the real-time observation data to develop the real-time hydro-logical forecasting model in most practical applications. The various adaptive techniques include the time series analysis, linear Kalman filter, multiple regression analysis, and statistical method. The real-time observation data including the rainfall, temperature, water stage, and soil moisture were employed in their models for subsequent forecasting.

Hydrologic models were frequently applied to the real-time flow discharge forecasting with adaptive techniques, but they lack the water stages and detailed flow information in a river basin. Hydraulic models can provide the detailed flow

information based on basic physical processes, but are unable to use the real-time data to adjust the flow. Hence, building a real-time flood-forecasting model by hydraulic routing is one of the most challenging and important tasks for the hydrologists. The purpose of this study is to develop a dynamic routing model with real-time stage correction method. The model should provide the real-time water stage for the significant locations in the river system and improve the accuracy of subsequent forecasting.

II. GEOGRAPHIC SETTING OF GODAVARI BASIN

Godavari basin extends over an area of 3, 12,812 sq kms, covering nearly 9.5% of total area of India. The Godavari River is perennial and is the second largest river in India. The river joins Bay of Bengal after flowing a distance of 1470 km (CWC 2005). It flows through the Eastern Ghats and emerges into the plains after passing Koida. Pranahita, Sabari and Indravathi are the main tributaries of Godavari River. (Fig 1). The basin receives major part of its rainfall during South West Monsoon period. More than 85 percent of the rain falls from July to September. Annual rainfall of the basin varies from 880 to 1395 mm and the average annual rainfall is 1110 mm. Floods are a regular phenomenon in the basin. Badrachalam, Kunavaram, and the deltaic portion of the river are prone to floods frequently. Perur and Koida gauge stations are the main base stations of the Central Water Commission for flood forecasting in the basin. Geographic setting and locations of these basin stations are shown in Figure 1[4]

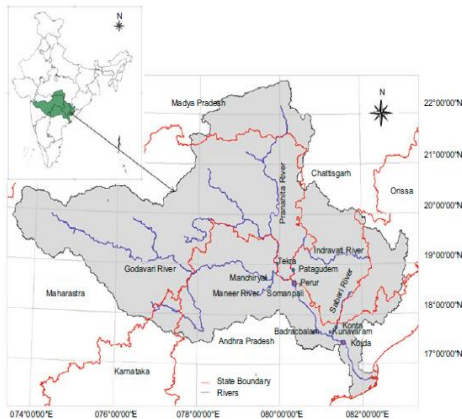


Fig. 1 Geographic setting of Godavari Basin [4]

III. FLOOD ROUTING

In hydrology, routing is a technique used to predict the changes in shape of water as it moves through a river channel or a reservoir. In flood forecasting, hydrologists may want to know how a short burst of intense rain in an area upstream of a city will change as it reaches the city. Routing can be used to determine whether the pulse of rain reaches the city as a deluge or a trickle. Flood routing is important in the design of flood protection measures, to estimate how the proposed measures will affect the behaviour of flood waves in rivers, so that adequate protection and economic solutions may be found.

Central Water Commission started flood-forecasting services in 1958 with the setting up of its first forecasting station on Yamuna at Delhi Railway Bridge. The Flood Forecasting Services of CWC consists of collection of Hydrological/ Hydro-meteorological data from 878 sites, transmission of the data using wireless/ fax/ email/ telephones /satellites /mobiles, processing of data, formulation of forecast and dissemination of the same. Presently, a network of 175 Flood Forecasting Stations including 28 inflow forecast, in 9 major river basins and 71 sub basins of the country exists. It covers 15 States besides NCT Delhi and UT of Dadra & Nagar Haveli. Central Water Commission on an average issues 6000 flood forecasts with an accuracy of more than 95% every year. [3]

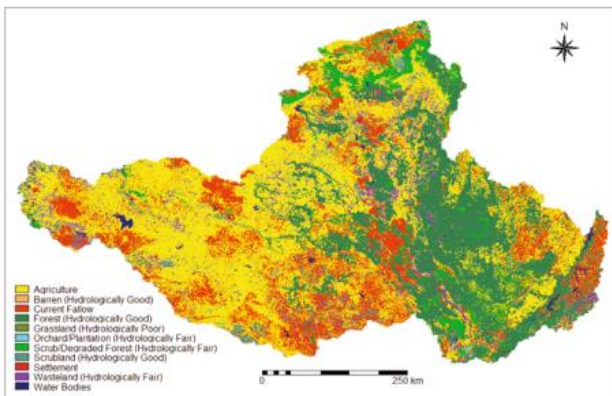


Fig. 2 Hydrological land covers of Godavari Basin

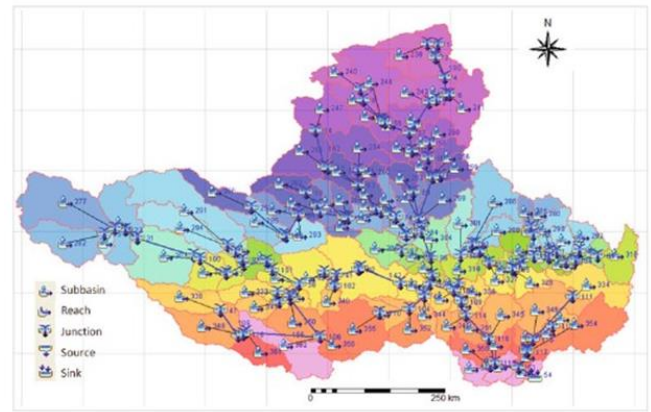


Fig. 3 Topographic model of Godavari Basin

IV. MODELING APPROACH AND METHODOLOGY

MIKE 11 is a professional engineering software tool for the simulation of hydrology, hydraulics, water quality and sediment transport in estuaries, rivers, irrigation systems and other inland waters. MIKE 11 is a modeling package for the simulation of surface runoff, flow, sediment transport, and water quality in rivers, channels, estuaries, and floodplains.

A. Hydrodynamic (HD) Module [1, 2]

The most commonly applied hydrodynamic (HD) model is a flood management tool simulating the unsteady flows in branched and looped river networks and quasi two-dimensional flows in floodplains. MIKE 11 HD, when using the fully dynamic wave description, solves the equations of conservation of continuity and momentum (known as the 'Saint Venant' equations). The solutions to the equations are based on the following assumptions:

- The water is incompressible and homogeneous (i.e. negligible variation in density)
- The bottom slope is small, thus the cosine of the angle it makes with the horizontal may be taken as 1
- The wave lengths are large compared to the water depth, assuming that the flow everywhere can be assumed to flow parallel to the bottom (i.e. vertical accelerations can be neglected and a hydrostatic pressure variation in the vertical direction can be assumed)
- The flow is sub-critical (super-critical flow is modeled in MIKE 11, however more restrictive conditions are applied)

The equations used are:

CONTINUITY:

$$\frac{\partial Q}{\partial x} + \frac{\partial A}{\partial t} = q$$

MOMENTUM:

$$\frac{\partial Q}{\partial t} + \frac{\partial(\alpha \frac{Q^2}{A})}{\partial x} + gA \frac{\partial h}{\partial x} + \frac{gQ|Q|}{C^2 AR} = 0$$

Where

- Q: discharge, (m³/s)
- A: flow area, (m²)
- q: lateral inflow, (m²/s)
- h: stage above datum, (m)
- C: Chezy resistance coefficient, (m^{1/2}/s)
- R: hydraulic or resistance radius, (m)
- I: momentum distribution coefficient

V. MODEL CALIBRATION AND VALIDATION

Model calibration is the process of adjusting model parameter values until model results match historical data. The process can be completed using engineering judgment by repeatedly adjusting parameters and computing and inspecting the goodness-of-fit between the computed and observed hydrographs. Significant efficiency can be realized with an automated procedure (U.S. Army Corps of Engineers 2001). The quantitative measure of the goodness-of-fit is the objective function. An objective function measures the degree of variation between computed and observed hydrographs. The key to automated calibration is a search method for adjusting parameters to minimize the objective function value and to find optimal parameter values. A hydrograph is computed at the target element (outlet) by computing all of the upstream elements and by minimizing the error (minimum deviation with the observed hydrograph) using the optimization module. Parameter values are adjusted by the search method; the hydrograph and objective function for the target element are recomputed. The process is repeated until the value of the objective function reaches the minimum to the best possible extent. During the simulation run, the model computes direct runoff of each watershed and the inflow and outflow hydrograph of each channel segment. The model computes the flood hydrograph at the outlet after routing flows from all sub basins to the basin outlet. The computed hydrograph at the outlet is compared with the observed hydrograph at all the sites.

A. Hydrodynamic (HD) Editor

The bed resistance is defined by a type and a corresponding global value. Local values are entered in tabular form at the bottom of the editor. There are three resistance type options:

1. Manning's M (unit: m^{1/3}/s, typical range: 10-100)
2. Manning's n (reciprocal of Manning's M , typical range: 0.010-0.100)
3. Chezy number.

The resistance number is specified in the parameter 'Resistance Number'. This number is multiplied by the water level depending 'Resistance factor' which is specified for the cross sections in the cross section editor (.xns11 files) to give a resulting bed resistance.

B. Initial Conditions

Initial conditions for the hydrodynamic model are specified on this page. The initial values may be specified as discharge and as either water level or water depth. The radio button determines whether the specifications are interpreted as water level or depth. The global values are applied over the entire network at the start of the computation. Specific local values can be specified by entering river name, chainage and initial values. Local values will override the global specification.

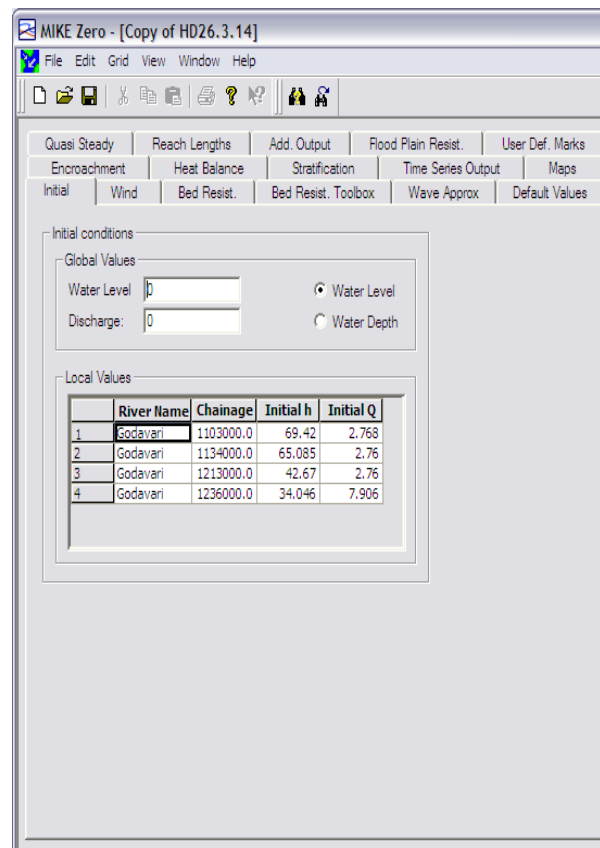


Fig. 4 Initial Conditions of Hydrodynamic Editor

C. Bed Resistance Toolbox

The bed resistance toolbox offers a possibility to make the program calculate the bed resistance as a function of the hydraulic parameters during the computation by applying a Bed Resistance Equation.

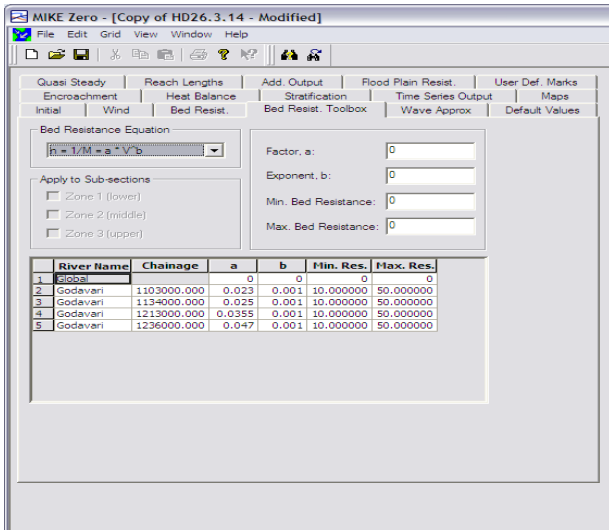


Fig. 5 Bed Resistance Toolbox of Hydrodynamic Editor

D. Surface and Root zone Parameters

The initial relative water contents of surface and root zone storage must be specified as well as the initial values of overland flow and interflow. Parameters used in surface and root zone are given below:

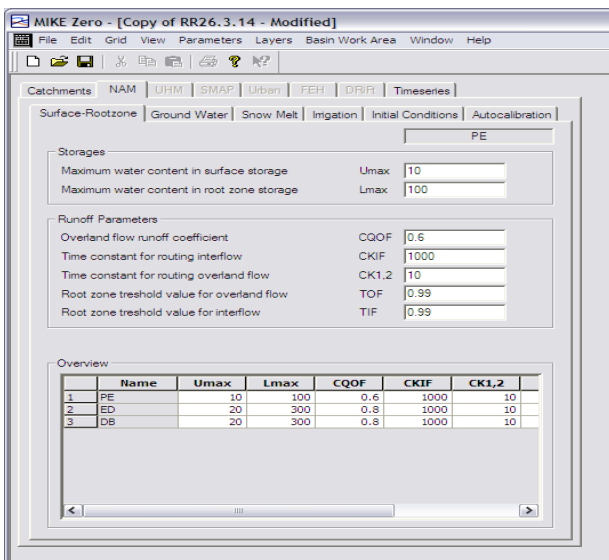


Fig. 6 Surface root zone parameters of Rainfall-Runoff Editor

The model is calibrated for the years 2009, 2010, 2011. After computing the exact value of the unknown variable during the calibration process; the calibrated model parameters are tested for another set of field observations to estimate the model accuracy. In this process, if the calibrated parameters do not fit the data of validation, the required parameters have to be calibrated again. Thorough investigation is needed to identify the parameters to be calibrated again. In this study, hydro meteorological data of 2012 were used for model validation.

VI. REAL TIME VALIDATION OF THE MODEL

The developed model has been validated thoroughly at the Central Water Commission Office in Hyderabad with the real-time hydro meteorological data during the floods of

2013 (the simulation period is 15 June to 15 October 2013). Considering the availability of real-time data, discharge data of the PERUR, Rainfall Data of Perur, Eturnagaram, Dummagudem and Badrachalam (Figure 1) were fed into the model as inputs. Rainfall runoff modeling was done in all the sub basins located in the study area down to the above mentioned stations. Hydrodynamic flow routing was also done in all the river channels. In real-time validation, the total flood routing stretch is approximately 133 km long (Perur to Badrachalam). The selected river reach Perur to Badrachalam is an ideal stretch as we have catchment area, flood routing, and a tributary joining in middle and the stretch is not very long, the intermittent catchment contribution is less. For study purpose this is the best stretch.

VII. RESULTS AND DISCUSSIONS

Agricultural land is the predominant land-use type in the study area that is severely exposed to floods every year. Slopes in the deltaic portion of the river are very flat (less than 3 percent), causing frequent inundation in this area. Soils in the study area are very fine in texture, resulting in more runoff.

The computed hydrograph during the validation process and observed hydrograph at Perur and Badrachalam stations are shown in Figures below.

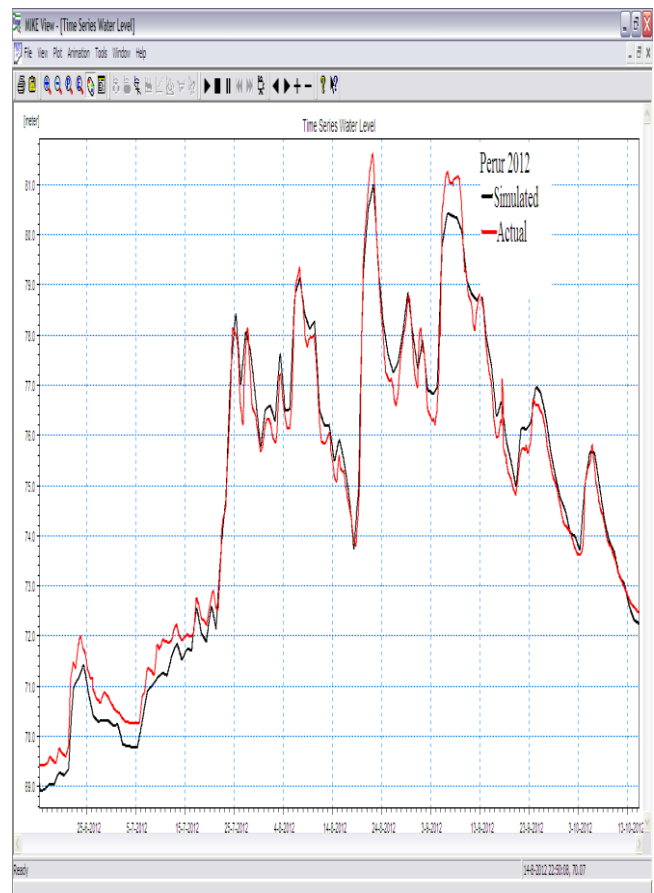


Fig. 7 Comparison of Actual Perur Water Level graph with the Simulated Perur Water Level graph for the year 2012

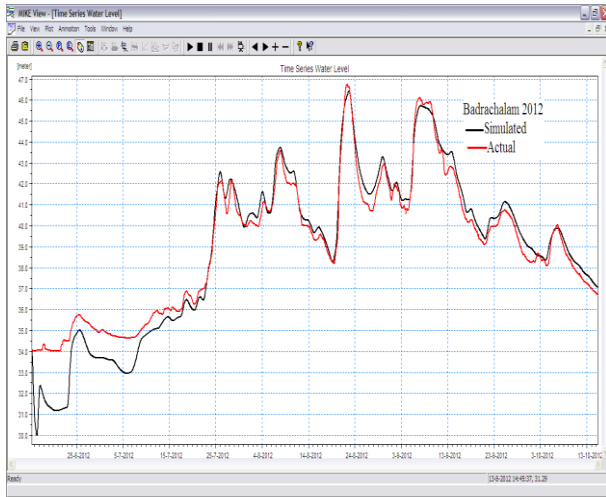


Fig. 8 Comparison of Actual Badrachalam Water Level graph with the Simulated Badrachalam Water Level graph for the year 2012

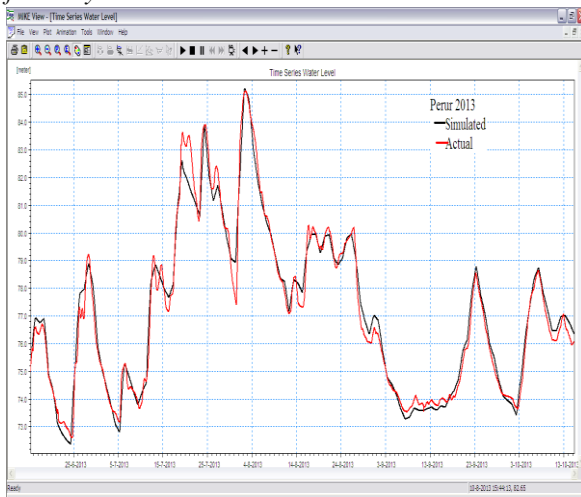


Fig. 9 Comparison of Actual Perur Water Level graph with the Simulated Perur Water Level graph for the year 2013

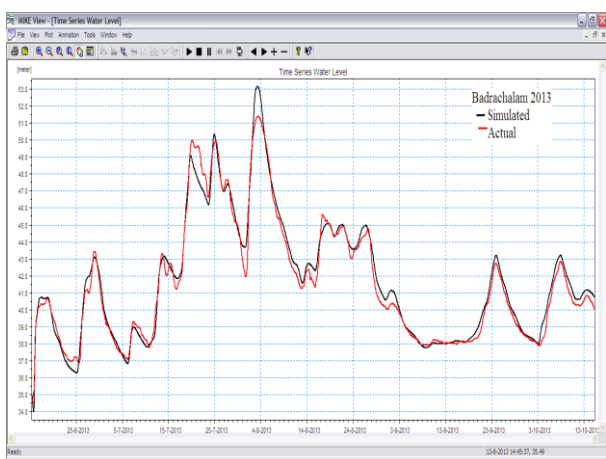


Fig. 10 Comparison of Actual Badrachalam Water Level graph with the Simulated Badrachalam Water Level graph for the year 2013

The computed hydrograph during the validation process and observed hydrograph at Perur and Badrachalam stations are shown in Figures. These figures indicate that the computed hydrographs match well with the observed hydrographs.

REFERENCES

- [1] Danish Hydraulic Institute (1994): MIKE 11 FF Short description: Real Time flood forecasting and modeling
- [2] DHI (2002) MIKE II: A Modeling System for Rivers and Channels. Reference Manual, DHI Software 2002, DHI Water & Environment, Horsholm, Denmark.
- [3] CWC (Central Water Commission of India). 1989. Manual on Flood Forecasting. New Delhi: Central Water Commission.
- [4] Korada Hari Venkata Durga Rao*, Vala Venkateshwar Rao, Vinay Kumar Dadhwal, Gandarbha Behera, and Jaswant Raj Sharma.,2011.A Distributed Model for Real-Time Flood Forecasting in the Godavari Basin Using special inputs.
- [5] Danish Hydraulic Institute (2003). MIKE 11 Reference Manual and User Guide, 2003 Ameen, M., Fang, C.S.,
- [6] 1970. Implicit flood routing in natural channel. Journal of Hydraulics Division, ASCE 96 (12), 2481–2500
- [7] Bairacharya, K., Barry, D.A., 1997. Accuracy criteria for linearised diffusion wave flood routing. Journal of Hydrology 195, 200–217
- [8] Bobinski, E., Mierkiewicz, M., 1986. Recent developments in simple adaptive flow forecasting models in Poland. Hydro- logical Sciences 31, 297–320.
- [9] Chow, V.T., Maidment, D.R., Mays, L.W., 1988. Applied Hydrology, McGraw-Hill, New York.
- [10] Chow, V.T., 1973. Open-Channel Hydraulics, McGraw-Hill, New York
- [11] David, C.C., Smith, G.F., 1980. The United States weather service river forecast system. Real-Time Forecasting/Control of Water Resource Systems, 305–325
- [12] Franchini, M., Lamberti, P., 1994. A flood routing Muskingum type simulation and forecasting model based on level data along Water Resources Research 30 (7), 2183–2196.
- [13] Jorgensen, G. H., and J. Host-Madsen. 1997. Development of a Flood Forecasting System in Bangladesh. In Proceedings of Conference



Study on GIS Simulated Water Quality Model

^[1]P.Lakshmi Sruthi, ^[2]P.Raja Sekhar, ^[3]G.Shiva Kumar

^[1]P.G.Student, ^[2]Associate Professor, ^[3]U.G.Student

^[1]kanchu1991@gmail.com, ^[2]sekharpr@yahoo.com, ^[3]shivakumar00740@gmail.com

Abstract— “A GIS-based watershed load model” which basically is the modeling of lake water quality by using geostatistical modeling techniques to understand the dynamics in a watershed. Simulation is illustrated through a case study for The Hussain sagar lake, Hyderabad which allows to the govern parameters of water quality like BOD, DO of lake water and phosphorus, nitrogen loads discharging into the lake from the primary influent streams. Results from the multi-layered geospatial model are expected to show a satisfactory coalescence between measured and simulated water parameters. This model enables prioritizing and effective management alternatives for protecting the water quality.

Index Terms—Compartment Model, ArcGIS Mapping, Water Characteristics, Data Sampling.

I. INTRODUCTION

The development of water quality models has reached an extremely important stage. Clean and Pure water is becoming more and more precious, although it is known that in absolute terms there is no 'clean water', in the management of water quality, we are trying to reduce the level of water pollution economically at the lowest possible cost. To achieve this goal, we perform a lot of numerical and statistical simulations to find out the best trade-off management solution. The final goal of using water quality management models is to simulate the consequences of different measures that can be taken to improve the water quality, and then to determine the measure which is optimal in both senses, economical and environmental [1]. Another major advantage of water quality models is that we can simulate different, even not quite well known, processes and the response of a physical system to certain forcing. By comparing the results of such simulations with field measurements and observations we can better understand physical, chemical and biological processes and find more accurate mathematical and statistical descriptions of these processes. Long-term continuous monitoring is not currently being conducted due to high costs. Therefore, there is a need for an alternate tool such as a basin-scale hydrologic/water quality model that is capable of predicting the effects with reasonable level of accuracy [2].

It is important that the right choice and use of numerical models can reduce to a minimum the number of necessary usually very expensive - field measurements. The Numerical water quality model is a complete integrated model for the simulation of water quality processes and transport, dispersion and the growth or decay processes of the relevant quantity (i.e. of a contaminant), through interaction with the biochemical processes.

Water Quality models can be zero-dimensional (generally compartment models), where complete mixing of all quantities inside the 'compartment' is assumed; one-dimensional, where subsequent connection of compartments is made (typically along a river reach); or two- or three-dimensional (2D, 3D) models. As the transport, dispersion of water parameters are considered on Lake Surface only 2D model will be discussed in this paper.

II. GEOGRAPHIC INFORMATION SYSTEM

A geographic information system (GIS) is a computerized database management system designed to capture, store, manipulate, analyze, manage, and present all types of geographical data and display of spatial (e.g. locationally defined) data. It digitally creates and "manipulates" spatial areas that may be jurisdictional, purpose, or application-oriented. The technology can be used to overlay and combine data into a single computerized map that can summarized geographic, cultural, and scientific land attribute.

GIS proving to be an effective tool for numerical models offers distributed parameter and continuous time simulation with flexible watershed configuration, inter-basin water transfer, and lake water quality simulation capabilities [4]. It has been proven to be an excellent tool to aggregate and organize input data for distributed parameter hydrologic/water quality models.

A GIS can be divided into five components: People, Data, Hardware, Software, and Procedures. All of these components need to be in balance for the system to be successful. No one part can run without the other. There are several things to consider before acquiring geographic data. It is crucial to check the quality of the data before obtaining it. Errors in the data set can add many unpleasant and costly hours to implementing a GIS and the results and conclusions of the GIS analysis most likely will be wrong.

Spatial modeling represents the structure and distribution of features in geographical space. In order to model spatial processes, the interaction between these features must be considered. There are several types of spatial data models including: vector, raster, surface, and network [11].

The vector data model is a method of storing and representing data on an X, Y Cartesian plane. A coordinate and an equation defining the curvature of each feature are stored for both the beginning and the end point of each feature. The building block of the vector structure is the point; lines and areas are composed of a series of points in a specific order that gives the object direction.

The raster data model uses a grid composed of rows and columns to display map entities. Each cell in the grid is equivalent to one map unit or one pixel. Spatial resolution determines the precision of spatial representation by raster

S.No	Nala & Location of I&Ds	Existing	Enhanced for projected
		Peak	Peak
1	Picketnala – Opp: Kims Hospital	15 MLD	171 MLD
2	Balkapur Channel	22 MLD	52 MLD
3	Yousufguda Nala near Divyashakthi Apartment	23 MLD	--
4	Bajara Nala near Yashoda Hospital	12 MLD	--
5	Kukatpally Nala at Fathenagar	75 MLD	185 MLD
6	Kukatpally Nala at Prakashnagar	30 MLD	44 MLD
7	Kukatpally Nala at Necklace Road (New)	-	100 MLD
Total		177 MLD	552 MLD

Establishments, Immersion of Ganesh and Durga Idols, Visitors and Tourists etc. Internal sources include Nutrient rich sediments on the lake bed and Floating matter on Lake Surface, Dissolved chemicals present in the deeper layers of the lake which do not have favorable conditions to diffuse out through the lake outlets.

B. Outlets

There are two outlets for Hussain Sagar Lake, They are - Surplus outlet opposite to Marriot Hotel and Surplus Outlet at Liberty. The location of inflows and Outflows of Hussain Sagar Lake are shown in Fig. 4.

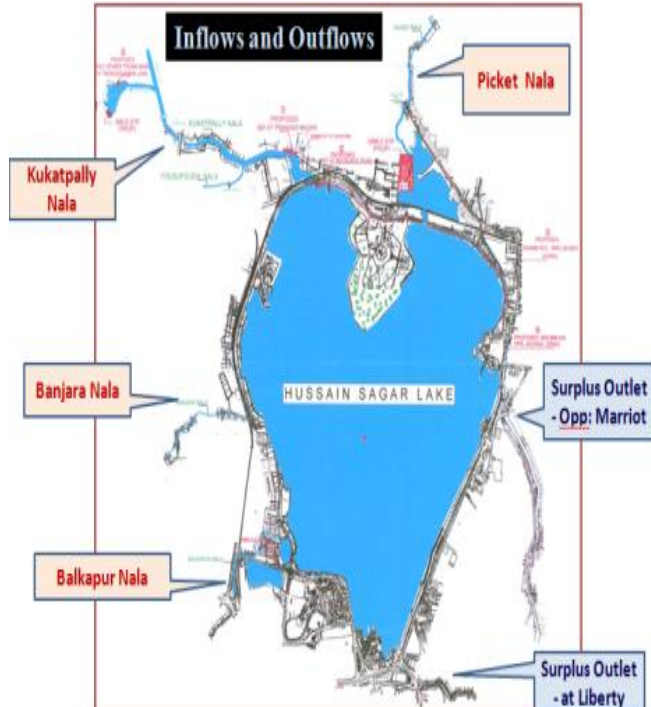


Fig. 4 Inlets and Outlets of Hussain Sagar Lake. (Color Print required)

TABLE I

INFLOW PEAK DISCHARGES AT DIFFERENT NALAS OF HUSSAIN SAGAR

MLD = Million litres per day; I & D = Interception and Diversion.

V. SAMPLING AND COLLECTION OF DATA

A total of 9 samples (as shown in Fig. 5) are collected at about the same time of each sampling day (at 9:30am) & the Sampling interval is taken as two weeks. The location of the sample collection points is fixed based on Periodical change in water level at the location and development of pressure around the point in the lake [6]-[7].

Sampling at shore, near inflows or in the windward direction where prevailing winds blow algae and debris down the lake and toward the sampling point is avoided. If collected, samples at these areas are less representative of the lake's overall water quality [3].

During sample collection, things recorded are the presence of storm water runoff culverts or pipes, types of shoreline vegetation (lawns, native vegetation, or agricultural land), Range of change in temperature, Probability of formation of shadow on the lake water surface due to adjacent structures and adjacent land use [3].

Characterization of wastes is essential for an effective and economical waste management programme [8]. It helps in the choice of treatment methods, deciding the extent of treatment, assessing the beneficial uses of wastes and utilizing the waste purification capacity of natural bodies of water in a planned and controlled manner.

The factors which contribute to variations in characteristics of the domestic sewage which comprises of spent water from kitchen, bathroom, lavatory, etc are daily per capita use of water, quality of water supply and the type, condition and extent of sewerage- system, and habits of the people. Municipal sewage which contains both domestic and industrial wastewater may differ from place to place depending upon the type of industries and industrial establishment.

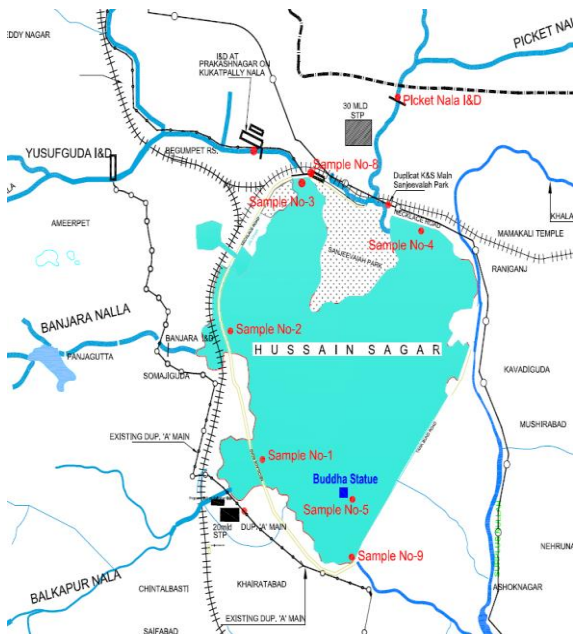


Fig. 5 Representation of all nine data sampling points (Color print required)

TABLE II

Lake water characteristics sampled on 22/07/13

Lake Water/Nala Water Analysis Report (22/07/13)

S.NO	Parameters	Units	Sample-1 Balkapur Nala at the joining point of lake	Sample-2 Banjara Nala at the joining point of lake	Sample-3 Kukatpally Nala at the joining point of lake	Sample-4 Picket Nala at the joining point of lake	Sample-5 Lake Water at Buddha Statue joining point of confluence	Sample-6 Jeedimetla Nala water before joining point of confluence	Sample-7 Kukatpally Nala water at Fathernagar after joining kukatpally and Jeedimetla nala	Sample-8 collection chamber of I&D necklace Road	Sample-9 Lake Water at Weir out let at BPPA office
1	pH	(-)	7.26	6.96	7.06	7.39	7.38	7.29	7.27	7.42	7.53
2	Temperature	°C	23	23	23	23	23	23	23	23	23
3	TDS	(mg/l)	598	617	732	708	633	1043	668	703	721
4	TSS	(mg/l)	18	29	31	24	17	56	33	21	18
5	DO	(mg/l)	0.8	Nil	Nil	Nil	0.7	Nil	Nil	Nil	0.9
6	Nitrates as N	(mg/l)	4.06	4.51	4.74	3.83	3.16	4.96	4.51	3.83	3.16
7	Ammonical Nitrogen as N	(mg/l)	8.4	12.28	15.32	8.28	5.86	10.82	11.8	9.56	8.82
8	Total Nitrogen as N	(mg/l)	13.26	17.72	21.14	12.9	9.92	16.62	17.18	14.3	12.8
9	Total Phosphorus as P	(mg/l)	1.88	2.11	2.4	2.18	1.2	1.55	1.22	1.38	1.09
10	COD	(mg/l)	62	86	124	96	74	118	78	66	70
11	BOD	(mg/l)	16	21	30	23	18	28	20	16	17

VI. DATABASE CONSTRUCTION AND EXPERIMENTATION

From the point samples (measurements), two continuous surfaces (maps) predicting the values of lake parameters or concentrations for every location within the boundary of lake were produced in Environmental Systems Research Institute's (ESRI) ArcGIS 9.0 which is the software used for visualization of the data and for map creation. The first map that is created will simply use all the default options to introduce you to the process of creating a surface from the sample points. A Digital Elevation Model (DEM) was obtained from the Geological Survey of India (GSI) in 1:50k in Digital format. Several DEM tiles were assembled to

attain a complete coverage of entire study area using MOSIAC command of Arc Info. The DEM was then REPROJECTED in Arc Info to the Universal Transverse Mercator (UTM) projection. The reprojected DEM was FILLED in Arc Info to correct to any internal drainage errors in the data layer. FLOWDIRECTION and FLOWACCUMULATION grids were derived from the DEM in Arc Info. Finally, the Hussain sagar Watershed was delineated using Arc Info's WATERSHED command. The last grid cell in the Hussain Sagar Lake before outlet to the Musi River was used as the pour point. The outlet of the watershed (pour point) was selected using the FLOWACCUMULATION grid. The second map that is produced will allow you to incorporate the assembled geo-spatial data to hussain Sagar lake boundary which is done using GRIDCLIP and CLIP commands of Arc Info. When creating this second map, the exploratory spatial data analysis (ESDA) tools are used to examine sample point data [10]. The database was compiled by obtaining data layer from a large number of sources. By using the ESDA tools and working with the geostatistical parameters, one can able to create a more accurate surface [5].

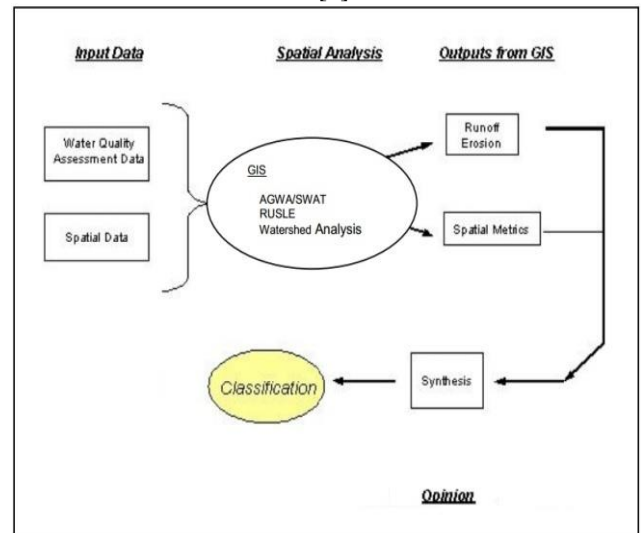


Fig. 6 Representation of experimentation procedure

The ca_lake.gdb (lake geodatabase file) is to be opened as in [9] which contain two datasets as

Dataset	Description
[1] ca_outline	[2] Outline of lake
[3] lake_points_9:30am	[4] point sample values (ppm)

Fig. 7 Datasets Included

The ESRI's Arc Info 7.2.1 and Arcview 3.3 were the GIS software programs used to integrate and process the data. All data layers were converted to the universal transverse mectator projection in ArcInfo. Data layers exist in ESRI's Coverage /Grid and Shapefile formats.

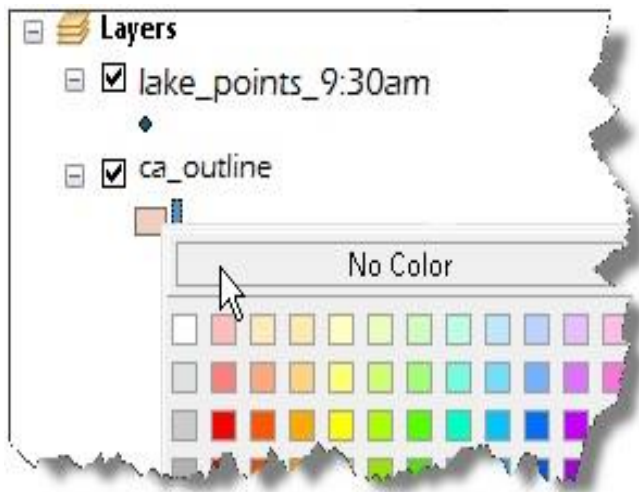


Fig. 8 Data Layers that are converted in to UTM Projection(Color print required)

Layers along with their properties (as in Fig. 8), Datasets (as in Fig. 7) are included into the software and the results obtained are in the form of a graph for the water parameters. Fig. 9 represents the obtained output, representing the simulation of water parameter i.e., BOD.

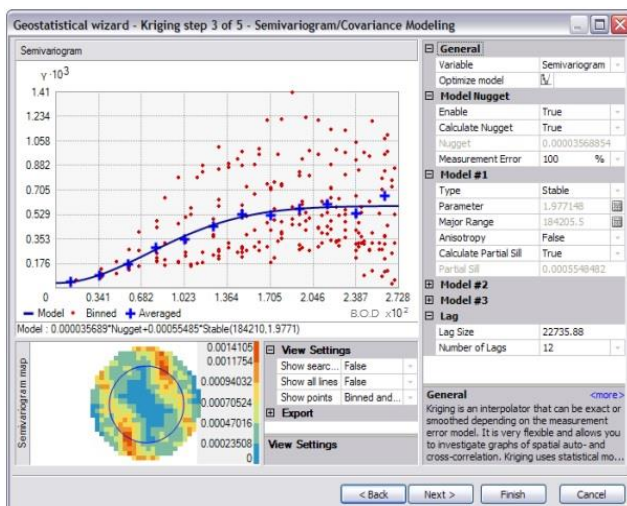


Fig. 9 Output obtained(Color print required)

The obtained output shown is water quality representation graph in terms of BOD. The values obtained from Model are shown as a blue line, the values sampled are shown as red dots and the averages of measured values are represented as blue plus symbols. The Modeled values are comparable and are approximately matching the sampled BOD values. As shown in Fig. 10, A cross validation check is done in the geostatistical wizard to check the quality of output from the simulation by calculating various prediction errors for all the samples measured values and model simulation output values.

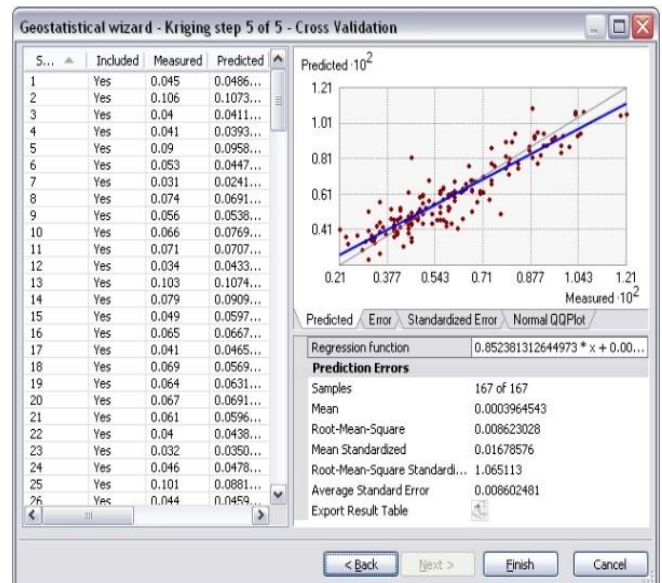


Fig. 10 Cross Validation of Simulation

As the Average standard error obtained (as shown in Fig. 10) is approximately zero, the model is eligible for usage in determining water quality parameters at any anonymous point on the lake surface.

REFERENCES

- [1] P.Sudha Rani TH 614.7: S94E (2004), Environmental monitoring of Hussain Sagar lake water, Hyd.
- [2] Krishna Kumar TH 591.5: K92E (1979), an ecological analysis of integration of ciliate protozoa and water quality fluctuations in lake hussain Sagar consequent influx of industrial effluent, OU, Hyd.
- [3] Executive Engineers of BPPA and APPCB, Hyd, A.P., India.
- [4] Peter A. Burrough, Prof. of physical geography, Principles of Geographical Information systems (1998).
- [5] He, C. 2003. Integration of geographic information systems and simulation model for watershed management. Environmental Modelling & Software 18: 809-813.
- [6] ADEQ, Arizona Department of Environmental Quality. 2003a. DRAFT Status of Water, Quality in Arizona – 2004: Arizona's Integrated 305(b) Assessment and 303(d) Listing
- [7] ADEQ, Arizona Department of Environmental Quality. 2003b. HUC Subwatershed Boundaries, Water Quality Sampling Datasets, and Designated Stream Reaches.
- [8] ADWR, Arizona Department of Water Resources. 2000. Verde River Watershed Study. Arizona Water Protection Fund, 500 North 3rd St., Phoenix, AZ 85004.
- [9] ALRIS, Arizona Land Resource Information System. 2002. Mines, Streams, and Landownership Datasets. <http://www.land.state.az.us/alris/alrishome.html>
- [10] Feoli, E., L.G. Vuerich, and W. Zerihun. 2002. Evaluation of environmental degradation in northern Ethiopia using GIS to integrate vegetation, geomorphologic, erosion and socio-economic factors. Agriculture, Ecosystems and Environment 91: 313-325.

- [11] Sheng, T.C., R.E. Barrett, and T.R. Mitchell. 1997. Using geographic information systems for watershed classification and rating in developing countries. *Journal of Soil and Water Conservation* (52)20: 84-89.
- [12] Sivertun, A., L.E. Reinelt, and R. Castensson. 1988. A GIS method to aid in non-point source critical area analysis. *International Journal of Geographical Information Systems* 2(4): 365-378.



Learning Experience In The Use Of Unity: Game Engine For Development Of 3d Expo

^[1] Tejal P. Rane, ^[2] Ashvini Madival, ^[3] Ningappa Arakeri, ^[4] Uttam Gouranna, ^[5] Priya Athani, ^[6] Priyadarshini D. Kalwad

^{[1][2][3][4][5]} Computer Science & Engineering Department, BVBCET, Hubli – 580031, India
^[1]tejalrane007@gmail.com, ^[2]ashviniaapsbmadival@gmail.com, ^[3]ningu145@gmail.com,
^[4]uttamg55@gmail.com, ^[5]priya.f671@gmail.com, ^[6]priyadarshini@bvb.edu

Abstract – The paper aims to introduce novel graphics software i.e. “Unity: Game Engine”. The software has revolutionized the world of game development by facilitating easy construction of games and their deployment into various popular platforms in current use. It can also be used by application developers to design impressive user interfaces for their projects. The software is known to provide exemplary assets via which it ensures ease of development. The document goes further to discuss the manner in which the authors have used Unity to develop the interface for their engineering capstone project i.e. 3D Expo.

Keywords – 3D Exposition (Expo), user interface, UnityEngine class, GUILayout class, GUISkin class.

I. INTRODUCTION

The domain of current discussion is computer graphics. This document intends to introduce Unity as a tool to empower the user to create the best interactive entertainment or multimedia experience. Unity is a cross-platform game engine with a built-in IDE developed by Unity Technologies. It is used to develop video games for web plugins, desktop platforms, consoles and mobile devices. It grew from an OS X supported game development tool in 2005 to a multi-platform game engine. The latest update, Unity 4.3, was released in November 2013. It currently supports development for iOS, Android, Windows, BlackBerry 10, OS X, Linux, web browsers, Flash, PlayStation 3, Xbox 360, Windows Phone 8 and Wii U. Two versions of the game engine currently in popular use are Unity and Unity Pro as in [1].

II. APPLICATIONS

A. Available Application

The sample game application available with the Unity set-up package is AngryBots. The interface design appears as shown below:

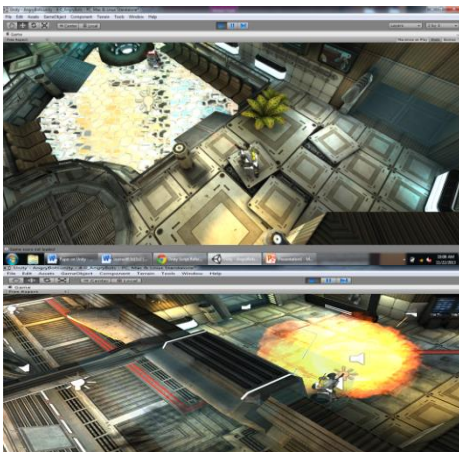


Fig. 1 User interface for AngryBots
Fig. 2 Player in action in AngryBots

AngryBots is a classic example of a gaming application developed using Unity. It emphasizes the advantages of Unity over other gaming software or interface development tools. As can be observed from the Fig. 1 and Fig. 2, Unity is able to achieve high definition scene rendering, with Mecanim being responsible for the fluid and natural motions of the characters.

B. Implemented Application

A sample application interface has been developed by the authors using the components available in the UnityEngine class for the software “3D Expo”. GUI and GUILayout are the classes used explicitly to include the various elements of the UI. They may be windows, buttons, labels or text fields. A snapshot taken at run time appears as below:



Fig. 3 User interface for 3D Expo
Fig. 4 A layout in 3D Expo

III. 3D EXPO

-The Graphics Presentation Tool

The aim of 3D Expo is to design and develop an intuitive, interactive and immersive framework where users can develop and present their thoughts in real time using computer graphics. It purports to develop an easy-to-use application dedicated solely to presenting 3D models, thereby overriding the popularity of existing tools which are very much complex in nature. Although these software provide facilities to actually create 3D designs, often they fail to serve their purpose because laymen find them incomprehensible.

The applications of 3D Expo will be observed in the following context:

- Widespread application of the tool may be seen in manufacturing industries where new designs need to be demonstrated to superiors and other members of the project teams.
- Education system may be enhanced by the use of this tool. Teachers will be able to showcase their lessons better and provide real time view of relevant examples.
- General users will be able to construct enhanced presentations in 3D as the tool will provide most of the features available in software in current use.

Here, the facilities provided by Unity are being put to use to develop the interface for 3D Expo. The GUI has been designed by classes available in UnityEngine. The GUI class offers various components required to develop an interface viz. windows, skins, menus, buttons, labels, text fields etc. The GUILayout class extends the features offered by the GUI class and enables self-alignment of interface elements.

Unity allows its users to develop exclusively new interfaces by creating custom windows of required dimensions and desired features. On the other hand, it also allows its users to modify the interface of Unity itself to suit their needs. This can be achieved using the GUISkin class. AngryBots uses this attribute of Unity for its interface. It can be observed in both Fig. 1 and Fig. 2 that the UI of AngryBots greatly resembles that of Unity with minor differences.

The assets available with Unity are of remarkable significance for novices in the field of computer graphics. Various 3D objects and behaviors can be added to the application by mere drag and drop options. For instance, the fires seen in the “Temple Run” games could be associated with any gaming applications by the simple act of importing the asset into the Unity project during development. The physics involved in the activity, say, the intensity of light emitted by the fire, the area covered, the smoke generated etc. can be easily manipulated within the project. Light sources of varied kinds are accessible like point lights, spot lights etc. The camera can be placed anywhere on the scene and can enable a 360 degree view of the 3D objects present. Material and response of surfaces to light incident on them too can be defined as specular, diffuse, ambient and likewise. Orientation of objects can be easily changed with the

available short-cuts. Furthermore, in order to view the effect of modifications at run-time, options are obtainable to preview the alterations with play, pause and stop options. Texture mapping which may prove to be quite complicated in computer graphics can be accomplished by simply placing the texture image on the object which needs to be textured. Unity thus facilitates graphics neophytes to play with various functions associated with computer graphics and thereby gain knowledge and understanding of the concepts involved.

Once the project executable is built, the application can be run by double clicking on the application icon. The default Unity icon can be replaced by custom icons as per the project requirement. The application begins with a Unity promo and there on proceeds to the actual application implementation.

The complete Unity software is available for download along with its free version at its home website, as in [1]. Once installed, a user can refer the “Unity Manual” and related documents which are available with the help options as in [3], [4] and [5]. They constitute a detailed instruction set elaborating how to use Unity along with its assets, shortcuts and scripting.

IV. EDUCATIONAL EXPERIENCE

There are several reasons why our team opted for Unity instead of the various other options available today. The design of our interface for 3D Expo is critical for its success. Presently, there are several software which have been in popular use for years now, and deal with 3D graphics or facilitate creation of 3D models or compile presentations. However there is no such tool which combines the features of all these and yet keeps the interface simple enough for user convenience. 3D Expo shall be unique because of its simplicity.

In order to achieve this, we needed a development tool which would make our programming task easy and let us focus on the usability and learnability of our interface. Unity: Game Engine was the one which answered our requirements. It provided us with all the facilities required to develop the application. In addition to this, it is a fairly easy tool to be learnt by fresh beginners. The developers have provided an excellent user manual detailing the use of every Unity feature and scripting construct.

The star feature of 3D Expo is the import of 3D models. Unity very adroitly aids this functionality at the back-end simplifying our work. In Unity itself, the importing of 3D models is an objectively easy chore. It allows us to search the system memory for compatible file formats, say .FBX, and add it as a component to the scene. Moreover, texturing of this object can be accomplished merely by importing the texture image and placing it on the object. We intend to follow this line of practice to allow the import functionality in our project.

It is to be noted that Unity is one of the very few tools which actually permits its users to modify its very own

interface to suit their needs. Using the GUISkin class we can add menu options, buttons, panels and the like to the basic interface window. For instance, assume that the developer wishes to add a new menu providing options to capture a camera footage, he can do so by assigning the string to corresponding property of the skin object. As most of the features provided by 3D Expo coincide with those of Unity, this property is going to prove highly beneficial for us in the course of our project development.

Additionally, Unity allows us to generate the executable file of our project along with all its assets segregated in a folder. All we need to do is click on the file menu, scroll down to build settings, choose the target platform & architecture and build it. We can put this to good use as we expect to develop a stand-alone application of our own. The Unity icon on the executable can be replaced by a custom icon of our own too.

As a result of these benefits we have decided on Unity as our development software. To our convenience, it allows us to do the scripting in C#, thus adding to its advantages those of C# too. The learning experience has been something really unexpected. It has been great fun to have accomplished the results of complex computer graphics programs by simple Unity routines. It was a surprise to learn so many among the popular games we have been enjoying have been developed with such ease using Unity. Moreover, Unity has made them available on several platforms. A part implementation of the Temple Run games was actually demonstrated to us by our guide in the matter of minutes. Our learning of the complete functionality of the Unity software is an ongoing process. By now, as far as our project development is concerned, it seems to be a promising venture.

V. CONCLUSION

At this point, one can infer that “Unity” is an innovation arrived right on time. With the ever changing and developing graphics world, programmers will find much use of tools like Unity to develop new applications to meet the customer demands. The authors have put in their best efforts to convey this fact to their readers.

ACKNOWLEDGEMENT

We acknowledge the role of Mr. Pavan Shinde of “Intuitive Education Systems – Redefining Education” in introducing us to “Unity”, as a tool to develop the interface for our engineering capstone project “3D Expo”. We express our heartfelt gratitude to our guides Asst. Prof. Priyadarshini D. Kalwad and Assoc. Prof. Vijayalaxmi M. of Computer Science & Engineering Dept. BVBCET, for their valuable guidance, co-operation and timely help.

REFERENCES

- [1] “Unity – Website”, <http://unity3d.com/unity>
- [2] “Unity: Game Engine”, [http://en.wikipedia.org/wiki/Unity_\(game_engine\)](http://en.wikipedia.org/wiki/Unity_(game_engine))
- [3] “Unity Manual”, <http://docs.unity3d.com/Documentation/Manual/index.html>
- [4] “Unity Reference Manual”, <http://docs.unity3d.com/Documentation/Components/index.html>
- [5] “Unity Scripting Reference”, <http://docs.unity3d.com/Documentation/ScriptReference/index.html>



Automatic Accident Detection With Traffic Light System

^[1] Atul Kumar, ^[2] Adeesh Sharma, ^[3] Girraj Sharma, ^[4] Amar Singh Rajak
^{[1][2][3][4]} B.E. , Dept. Of E.I.E. , Institute of technology and management , Gwalior(M.P.)
^[1]kanchu1991@gmail.com, ^[2]sekharpr@yahoo.com, ^[3]shivakumar00740@gmail.com

Abstract: Now days the road accidents in modern urban areas are increased to uncertain level. The loss of human life due to accident is to be avoided. Traffic congestion and tidal flow are major facts that cause delay to ambulance. To bar loss of human life due to accidents we introduce a scheme called ITLS (Intelligent Traffic Light system). The main theme behind this scheme is to provide a smooth flow for the emergency vehicles like ambulance to reach the hospitals in time and thus minimizing the delay caused by traffic congestion. The idea behind this scheme is to implement ITLS which would control mechanically the traffic lights in the path of the ambulance. The ambulance is controlled by the control unit which furnishes adequate route to the ambulance and also controls the traffic light according to the ambulance location and thus reaching the hospital safely. The controller identifies the location of the accident spot through the sensor systems in the vehicle which determined the accident and thus the controller walks through the ambulance to the spot. This scheme is fully automated, thus it finds the accident spot, controls the traffic lights, helping to reach the hospital in time.

Keywords: ITLS, Traffic, Congestion, Sensor system

I. INTRODUCTION

Nowadays Wireless Sensor Networks (WSN) has been applied in various domains like weather monitoring, military, home automation, health care monitoring, security and safety etc. or in a nut shell one can say wireless sensor network can be applied in most of the domains. Traffic Signal System or traffic monitoring is a vast domain where WSN can be applied to gather information about the incoming flow of traffic, traffic load on a particular road, traffic load at particular period of time (peak hours) and in vehicle prioritization. WSN installed along a road can be utilized to control the traffic load on roads and at traffic intersections.

The sensor nodes that are to be deployed along the road are small in size and have low energy consumption. These sensors run on both battery power as well as solar energy. They have the capability to draw solar energy so that they can use sunlight for functioning in bright and sunny condition and the battery power for functioning at night or in cloudy or foggy condition. Sensors used in the Wireless Sensor Network for traffic signal systems are mainly of two types: i) Intrusive type and ii) Non-Intrusive type. i) Intrusive types of sensor are kept under the road and sense the traffic waiting at the signal. This type of sensor has the same working principle as that of a metal detector. ii) Non-Intrusive types of sensor is fitted on the road. The installation of this type of sensor is easy as no cutting of road is needed to be done. Non-intrusive sensor includes acoustic sensors or video image processors to detect the presence of vehicles waiting at the traffic intersection. Although Intrusive sensors are very effective still Non-intrusive sensors are preferred over Intrusive sensors as they are cost-effective, easy to install, immune to natural corrosion and degradation.

II. PROPOSED SYSTEM

In proposed system if a vehicle has met accidents, immediately an alert message with the location coordinates is sent to the Control center. From the control center, a message is sent to the nearby ambulance. Also signal is transmitted to all the signals in between ambulance and vehicle location to provide RF communication between ambulance and traffic section. The vehicle accident observed using vibration sensor and in the control section it is received by the microcontroller and then the nearby ambulance is received from the PC and controller sends the message to the ambulance. The signal to Traffic signal section is transmitted through RF communication. Also if any fire occurs, it is detected using fire sensor and an alarm message is directly sent to the fire station.

III. BLOCK DIAGRAMS

A . Block Diagram Of Vehicle Unit

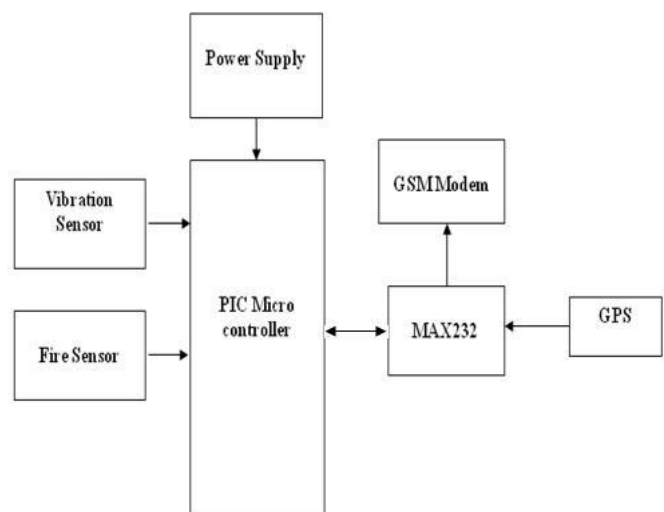


Fig.1 Block diagram of vehicle unit

If a vehicle has met accident, vibration sensor or fire sensor gives the electric signal to microcontroller through signal conditioner. Then GPS provides latitude and longitude information about vehicle location to control section through GSM.

B. Block Diagram Of Ambulance/Control Unit

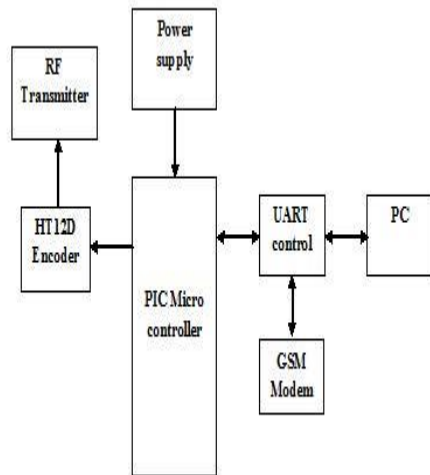


Fig.2 Block Diagram of Ambulance/Control Unit

In control section GSM modem receives message about accident and send it to PC. PC identifies the nearest ambulance and ambulance is instructed to pick up the patient. Control section transmits the control signal to all the signals in between ambulance and vehicle by RF transmission.

C. Block Diagram Of Traffic Unit

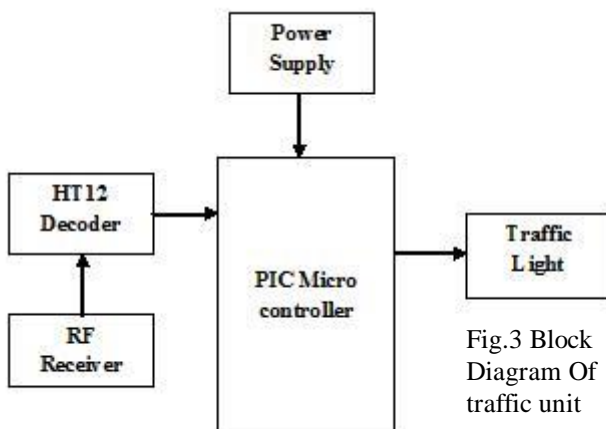


Fig.3 Block Diagram Of traffic unit

Whenever the ambulance reaches near to the traffic signal(approximately 100m), the traffic signal will be made to green through RF communication. Thereby the ambulance is recommended to reach the hospital in time.

IV. SYSTEM IMPLEMENTATION

Our system consists of three main units, which coordinates with each other and makes sure that ambulance reaches the hospital without any time lag. Thus our system is divided into following three units,

- The Vehicle Unit
- The Ambulance/control Unit
- Traffic unit

A. Vehicle unit

The vehicle unit installed in the vehicle senses the accident and sends the location of the accident to the controller. According to our system, every vehicle should have a vehicle unit. The vehicle unit consists of a vibration sensor, controller, siren, a user interface, GPS system and a GSM module. The vibration sensor used in the vehicle will continuously sense for any large scale vibration in the vehicle [1]. The sensed data is given to the controller GPS SYSTEM inside the vehicle. The GPS SYSTEM finds out the current position of the vehicle (latitude and the longitude) which is the location of the accident spot and gives that data to the GSM MODULE. The GSM MODULE sends this data to the control unit whose GSM number is already there in the module as an emergency number

B. Ambulance unit

The controller finds the nearest ambulance to the accident spot and also the shortest path between the ambulance, accident spot and the nearest hospital. The controller then sends this path to the ambulance. Also using this information the controller controls all the traffic signals in the path of ambulance and makes it ready to provide free path to ambulance, which ensures that the ambulance reaches the hospital without delay. At the same time, the ambulance unit turns ON the RF transmitter. This will lead to communicate with the traffic section.

C. Traffic unit

Whenever traffic signal section receives the information about accident, the RF receiver in this section is turned ON to search for ambulance nearing the traffic signal. Whenever the ambulance reaches near to the traffic signal(approximately 100m), the traffic signal will be made to green through RF communication. Thereby the ambulance is recommended to reach the hospital in time.

V. CONCLUSION

In this paper, a novel idea is proposed for controlling the traffic signals in favor of ambulances during the accidents. With this system the ambulance can be maneuvered from the ITLS can be proved to be effectual to control not only ambulance but also authoritative vehicles. Thus ITLS if implemented in countries with large population like INDIA can produce better results. The ITLS is more accurate with no loss of time. But there may be a delay caused because of GSM messages since it is a queue based technique, which can be reduced by giving more priority to the messages communicated through the controller.

VII. REFERENCES

1. Greater Amman Municipality, "Traffic report study 2007," <http://www.ammancity.gov.jo/arabic/docs/GAM4-2007.pdf>.
2. The Vehicle Detector Clearinghouse, "A summary of vehicle detection and surveillance technologies used in intelligent transportation systems," Southwest Technology Development Institute, 2000.
3. Minnesota Department of Transportation, "Portable non-intrusive traffic detection system," networks for monitoring traffic," in *Proceedings of the 42nd Annual Allerton Conference on Communication, Control, and Computing*, 2004, pp. 32-40.
4. S. Coleri, S. Y. Cheung, and P. Varaiya, "Sensor
5. I. F. Akyildiz, W. Su, Y. Sankarasubramaniam, and E. Cayirci, "A survey on sensor networks," *IEEE Communications Magazine*, Vol. 40, 2002, pp. 102-114.
6. A. N. Knaian, "A wireless sensor network for smart roadbeds and intelligent transportation systems," Technical Report, Electrical Science and Engineering, Massachusetts Institute of Technology, June 2000.



A Design and Simulation of Optical Pressure Sensor based on photonic crystal in Sub-Micron Range

^[1] Rajeshwari S, ^[2] Indira Bahaddur, ^[3] Dr. Preeta Sharan, ^[4] Dr. P C Srikanth

^[1] Department of ECE, Malnad College of Engineering, Hassan, India,

^[2] Department of ECE, Assistant Professor, Malnad College of Engineering, Hassan, India

^[3] Department of ECE, Professor, The Oxford College of Engineering, VTU, Bangalore, India

^[4] Department of ECE, Professor, Malnad College of Engineering, Hassan, India

Abstract: MOEMS based micro-sized pressure sensor can be developed to detect even sub-micron range dimension change using the photonic crystal. The applied pressure on the object will change the dimension of the waveguide carved in the photonic crystal. As a result, this change in spacing can alter the propagation feature of electromagnetic waves that pass through them that is changing the transmission spectrum. So, this change can directly be mapped to pressure on the observed object. In this paper, the pressure sensor using photonic crystal has been modeled and analyzed.

Keywords: FDTD, MOEMS, Micro-optics, Photonic crystal, Photonic sensing technology, Pressure Sensor

I. INTRODUCTION

Integrated photonics has opened a way to develop sensor systems which can replace the conventional electronic pressure sensors. The miniaturization, extreme efficiency and high sensitivity has made photonic sensor most viable solution to the conventional pressure sensor with limitations like inefficiencies in harsh environment, high cost and low sensitivity. Opto-mechanical micro sensor technology can be explored to develop pressure sensor. MEMS merged with Micro-optics involves sensing or manipulating optical signals on a very small size scale using integrated mechanical, optical, and electrical systems, giving rise to a new class of MOEMS technology.

Photonic sensing technology is innovative approach to identify and measure physical variables. Photonic crystal is array of periodic change in refractive index which can engineer the flow of light passing through it. The slightest change in the arrangement of index of refraction and corresponding dimension alters the transmission spectrum, which provides the photonic crystal very sensitive detection capability. Stable alignment, thermal stability, low cost, low energy requirement, faster response and compatibility with fiber-optic cable makes photonic sensor for pressure sensing have applications in various field from structural health monitoring, underwater applications, bio-medical applications to aerospace engineering.

In this paper, we propose a model for photonic crystal based pressure sensor. The model consists of a waveguide carved in two dielectric slabs surrounded by photonic crystal. The dielectric slabs are mobile. The photonic crystal is mounted on the object under observation. As such its pressure can be coupled to the movement of the dielectric slabs in the photonic crystal and pressure variation can be mapped to the separation of these slabs and thus measured.

As a consequence the optical properties of the photonic crystal like the transmission spectrum change. The altered transmission spectrum act as a signature of the pressure applied. The spectral analysis has been done to detect the change in the pressure.

II. THEORY

The photonic crystal is defined as periodic profile of refractive index which allows the controlled flow of the light through it. The artificial photonic crystal structures can be fabricated using immensely developed CMOS technology. It appears in one-dimension, two-dimension and three dimensions. It exists in two configurations: rods in air configuration and holes in slab configuration. The photonic crystal appears in different lattice structures example square lattice and hexagonal lattice. In this paper, two works are carried out. One is using two-dimensional square lattice photonic crystal with rods in air figuration and another is using two-dimensional hexagonal lattice photonic crystal with holes in slab configuration.

The defect engineering is an important aspect of the photonic crystal which is responsible for the controlled propagation of light through it. Defect engineering is the controlled change in the index profile of the photonic crystal to modify course of the electromagnetic waves passing through it. The line defect and point defect are the two types of defect popularly used and are very useful for creating band gap structures for different applications.

The photonic band gap property can be explored for the sensing applications. The band gap is referred to as an optical insulator. The bandgap property is precisely dependent on the refractive index arrangement of the photonic crystal. The smallest change in the refractive index profile example change in radius of holes or change

in the dimension of the waveguide, there is a precise change in the band gap property. Thus the band gap structures are efficient and highly sensitive sensor devices.

FDTD(Finite Difference Time Domain) Method: FDTD method provides a solution to Maxwell's equation. In FDTD method a finite rectangular grid is divided into space and time. These equations are solved using MEEP simulation tools. MEEP implements FDTD method to compute transmission spectrum.

The model of photonic crystal consist waveguide carved with the help of two dielectric slabs, with the upper plate mobile. As the pressure is applied on the photonic crystal, the dielectric slab moves and change the dimension of the waveguide. As a result the index profile of the photonic crystal is altered and thus changing the spectral property. This change in optical property is directly proportional to the applied pressure.

III. DESIGNS

1. Pressure sensor using rods in air configuration photonic crystal:

The first design of Pressure sensor is a two dimensional, square lattice photonic crystal with a line defect in rods in air configuration. The model consists of waveguide carved with the help of two dielectric slabs. The upper dielectric slab is mobile with respect to the pressure applied.

Following points explain the design parameters of the modeled pressure sensor:

- Rods in air configuration.
- Radius of rods $0.17\mu\text{m}$.
- Square Lattice.
- Lattice constant ' a '= $1\mu\text{m}$.
- Dielectric constant of dielectric slab is 11.56.
- The length of each plate is $10\mu\text{m}$ and width is $1\mu\text{m}$.
- Dielectric constant of the waveguide is 1 (Air).
- Height of slab is infinity
- Light source: Unit Gaussian Pulse with center frequency at 0.4, width of the pulse is 0.3.
- Minimum distance between dielectric slabs is zero μm and the maximum distance between dielectric slabs is $2\mu\text{m}$

The structure of the design-1 model is illustrated in the Figure 1 with maximum separation and figure 2 with minimum separation between dielectric slabs.

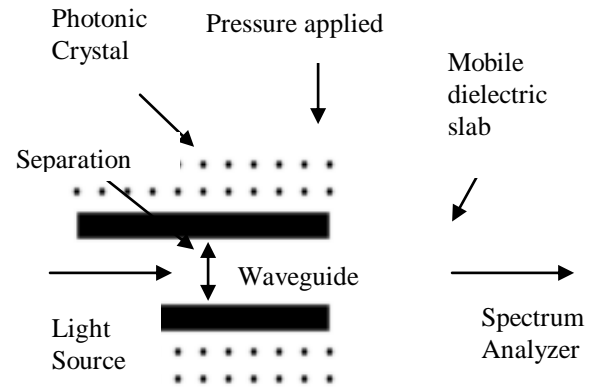


Figure 1: Model of the pressure sensor (rods in air configuration)

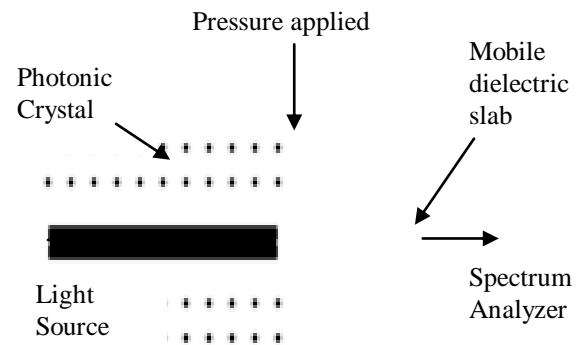


Figure 2: Model of the pressure sensor with minimum separation (rods in air configuration).

2. Pressure sensor using holes in slab configuration photonic crystal:

The second design of Pressure sensor is a two dimensional, hexagonal lattice photonic crystal with a line defect in holes in slab configuration. The model consists of waveguide carved with the help of two dielectric slabs. The upper dielectric slab is mobile with respect to the pressure applied.

Following points explain the design parameters of the modeled pressure sensor:

- Holes in slab configuration.
- Holes in slab $0.40\mu\text{m}$.
- Hexagonal Lattice.
- Lattice constant ' a '= $1\mu\text{m}$.
- Dielectric constant of dielectric slab is 11.56.
- The length of each plate is $10\mu\text{m}$ and width is $1\mu\text{m}$.
- Dielectric constant of the waveguide is 1 (Air).
- Height of slab is infinity
- Light source: Unit Gaussian Pulse with center frequency at 0.4, width of the pulse is 0.3.

- j) Minimum distance between dielectric slabs is zero μm and the maximum distance between dielectric slabs is $0.5\mu\text{m}$

The structure of the design-2 model is illustrated in the Figure 3 with maximum separation and figure 4 with minimum separation between dielectric slabs.

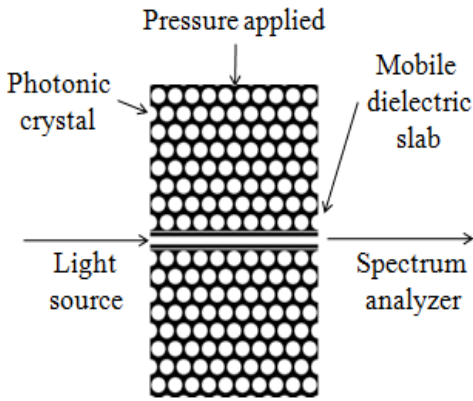


Figure 3: Model of the pressure sensor (holes in slab configuration)

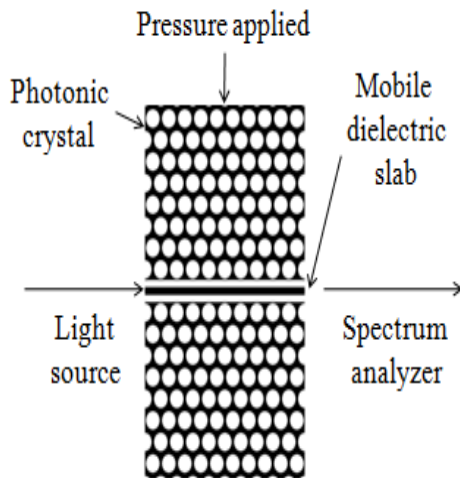


Figure 4: Model of the pressure sensor with minimum separation (holes in slab configuration).

The modeling and simulation has been done with the help of MEEP simulation tool. MEEP tool works in time domain and provides implementation of Finite Difference Time Domain Method. MEEP is MIT Electromagnetic Equation Propagation. MEEP is 'dimensionless' tool where μ_0, ϵ_0, c are unity. The output of MEEP is the transmitted power; the transmission spectrum is obtained using output from MEEP.

Operation: The Gaussian light pulse is passed through one end of the photonic crystal while the spectrum analyzer

is placed in the other end. The applied pressure moves the mobile plate reducing or increasing the distance between two dielectric slabs. The movement of the plate is considered in 20 steps, each step of $0.1\mu\text{m}$ for design1 and for design2 we have considered in 5 steps, each step of $0.1\mu\text{m}$. The changed dimension of the waveguide alters the light propagation and thus changing the transmission spectrum. The transmission spectrum is observed at each step of $0.1\mu\text{m}$ increase or decrease in distance between the two dielectric slabs.

IV. RESULTS

The transmission spectrum is plotted as shown in figure 5 given below.

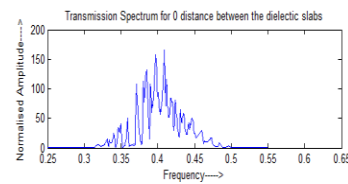


Figure 5: The transmission spectrum for zero separation between the dielectric slabs in design-1.

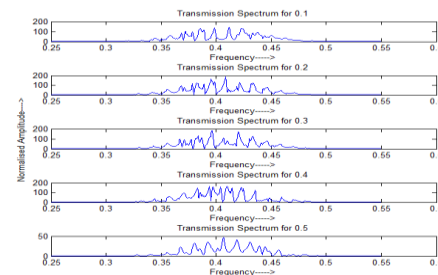


Figure 6: The transmission spectrum for 0.1, 0.2, 0.3, 0.4, 0.5 dimension(μm) of the waveguide in design-1.

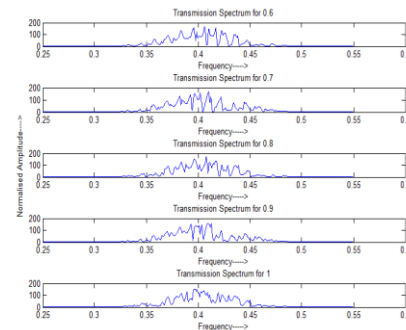


Figure 6: The transmission spectrum for 0.6, 0.7, 0.8, 0.9, 1 dimension (μm) of the waveguide in design-1.

Figure 7: The transmission spectrum for 1.1, 1.2, 1.3, 1.4, 1.5 dimension (μm) of the waveguide in design-1.

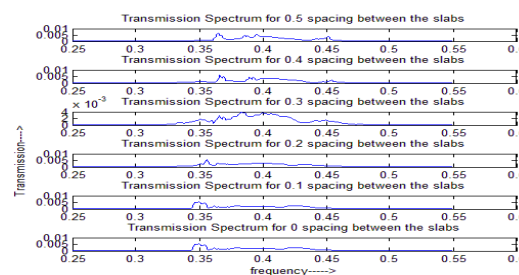
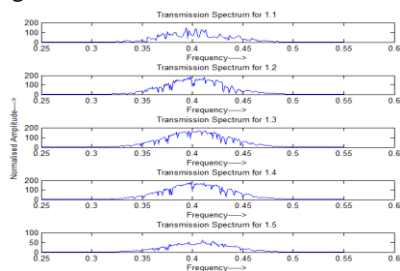


Figure 8: The transmission spectrum for 1.6, 1.7, 1.8, 1.9, 2 dimension (μm) of the waveguide in design-1

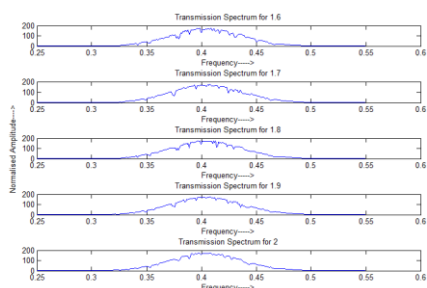


Figure 9: The transmission spectrum for 0.5, 0.4, 0.3, 0.2, 0.1, and 0 dimension (μm) of the waveguide in design-2.

V. CONCLUSION

In this paper, we are successful in modeling and analyzing pressure sensor using photonic crystal in sub-micron range. The varying spectrum of the waveguide can suitably and efficiently represent and measure pressure applied on the object. Further, it can be designed and fabricated to measure expansion or compression or both.

REFERENCES

- [1] An article 'Recent advancement in sensor technology for underwater environment' by Mohd

Rizwal Arsad, Indian Journal Of Marine Sciences, Vol. 38(3), September 2009, pp. 267-273

[2] 'Optical Fiber Sensor for Chemical Detection', US patent number 4834496, May 30, 1989

[3] 'Sensor Device', by Mitsuro Sugita, US patent number US7391945, 2008

[4] 'Two-Dimensional Photonic Crystal', by Susumu Noda et al. US patent number US7853111B2, 2010

[5] http://abinitio.mit.edu/wiki/index.php/Meep_Introduction/Transmission.2Freflection_spectra

[6] 'Photonic Crystals: Modeling The Flow Of Light', by John D. Joannopoulos, Steven G. Johnson, Robert D. Meade.

[7] 'A Novel Method for Switching and Tuning of PBG Structures', Jack Wu, S. N. Qiu, C. X. Qiu, 2 and I. Shih, Department of Electrical and Computer Engineering McGill University, 2004.

[8] 'Photonic Crystals: Modeling The Flow Of Light', by John D. Joannopoulos, Steven G. Johnson, Robert D. Meade.

[9] http://en.wikipedia.org/wiki/Photonic_crystal#Fabrication_challenges

[10] <http://ab-initio.mit.edu/MEEP/Tutorial>.

MEMS Based Optical Sensor for Salinity Measurement

^[1]Shruthimala N S, ^[2]Indira Bahaddur, ^[3]Dr. Preeta Sharan, ^[4] Dr. P C Srikanth

^[1]Department of ECE, Malnad College of Engineering, Hassan, India

^[2]Department of ECE, Assistant Professor, Malnad College of Engineering, Hassan, India

^[3]Department of ECE, Professor, The Oxford College of Engineering, Bangalore, India

^[4]Department of ECE, Professor, Malnad College of Engineering, Hassan, India

Abstract: In this paper, we propose a two dimensional photonic crystal based optical sensor for salinity measurement. The salinity percentage of sea water changes as we go down the sea water surface. This gives change to the index of refraction of the sea water at the different levels. Thus the salinity percentage of sea water can be detected by measuring this change in the effective refractive index of sea water. In this paper, the effective refractive index method has been used for the detection of the salinity concentration from (0-40%). The slab waveguide is designed and the effective refractive index change is captured. Even as the refractive index change for the change in salinity of the sea water, is very small, the effective index change is visible, making the sensor very sensitive.

I. INTRODUCTION

The photonic sensing technology has emerged as the innovative technique to explore the complicated system such as underwater environment. The underwater environment is difficult to explore since it presents uncertain conditions and difficult monitoring and measurement conditions. The corrosive nature of sea water, uncertain pressure conditions and very scarce source of energy impose difficulties for sensing and monitoring sea water environment. The photonic sensing technology provides ways to overcome these limitations and enable sensing and monitoring of the underwater environment.

Conventional way of measuring the salinity of a solution is to use a portable conductivity meter (EC meter)[1]. This enables instantaneous salinity readings to be obtained. The 'electro-conductivity' of the solution increases with the concentration of the salts. The common troubles in obtaining good results with conductivity monitoring equipment are linked to electrode fouling and insufficient sample circulation. The photonic crystal based sensor provides solution to the problems of salinity measurement. This optical sensor promises to be cheap and easy to manufacture, essential features for an replaceable probe.

In this paper, we propose a two dimensional photonic crystal based optical sensor using the effective refractive index method for salinity percentage detection in the sea water.

II. THEORY

The optical sensor's ability to act as a sensor for salinity measurement is based on the fact that the different levels of sea water samples have refractive index as the salinity concentration change. As a result, the change in index of refraction modifies the propagation of electromagnetic waves that pass through the photonic crystal. Thus, the salinity concentration can be detected by capturing the change in

refractive index. The different methods employed in photonic sensing technology are fluorescence, optical imaging, spectroscopy, band gap method, effective index and other methods.

In this paper, the effective index method is used for the sensing of the salinity which is simple and efficient to implement.

The slab waveguide is used in this method and a layer of sample is applied to over the waveguide. The applied sample of sea water changes the light propagation through the slab waveguide, thus changing the overall index of the waveguide. As a result, by detection of the overall refractive index of the waveguide the change in salinity can be observed. In these structures, the guidance is nearly a slab waveguide in one dimension with a small perturbation to index or core thickness that achieves guidance in the other dimension.

The effective index method begins by analyzing the structure for each segmented slab waveguide section and assigning effective indices for each section. Next, the effective indices for each slab segment are used to solve for the resulting slab waveguide geometry in the slightly perturbed dimension [4].

III. DESIGN

The slab waveguide design is shown in figure 1. Using the dispersion equation [7], the dispersion curve can be obtained. By using the dispersion curve equation the effective index value is calculated. In this project the photonic crystal is placed at the core of the slab waveguide.

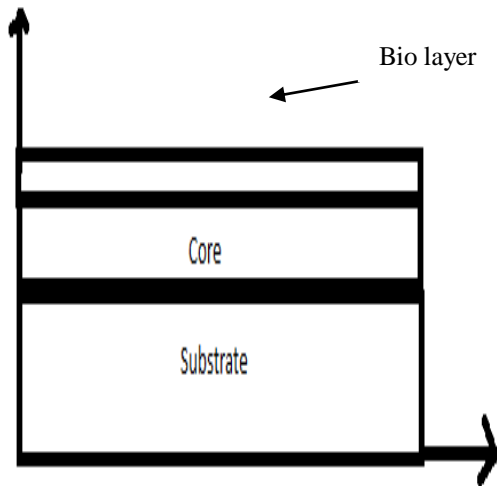


Figure: Slab waveguide

Photonic crystal is an optical analogue to the crystal structure of electronic materials. In the crystal structure, in conventional electronic materials, the atoms and molecules are periodically arranged. In photonic crystal the atom and molecules are replaced by macroscopic media with differing dielectric constants, and the periodic potential is replaced by a periodic dielectric function.

The band structure obtained for the photonic crystal help to determine the effective refractive index of the core. The slope the band is calculated from the band diagram obtained and the inverse of slope is the group velocity. The group index is nothing but the speed of light divided by group velocity. This group index of photonic crystal is used instead of core in the slab structure and thus calculating the effective refractive index.

Source code for modeling and designing of photonic crystal waveguide is developed with MEEP and MATLAB software. The MEEP tool uses scripting language and the simulation is carried out by this tool. This tool is used for finding the field distribution of electromagnetic wave.

IV. RESULTS

The frequency values, constitutes the band structure, is obtained as one of the output of MEEP design. After the calculations, the effective index values are obtained. These values are then plotted using MATLAB to obtain the change is refractive index against effective index, shown in Figure 2. From the figure 2, it can be observed that even for the slightest change in refractive index, the change in the effective index in more, making the designed sensor highly sensitive and selective.

In figure 3, the percentage salinity is plotted against the effective index. It can be observed from the figure that the effective index decreases exponentially as the salinity increases.

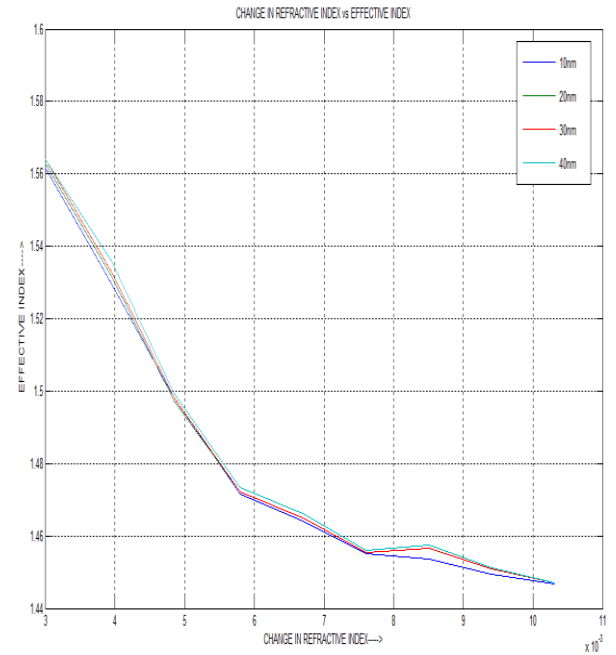


Figure 2: Change is Refractive Index against Effective Index

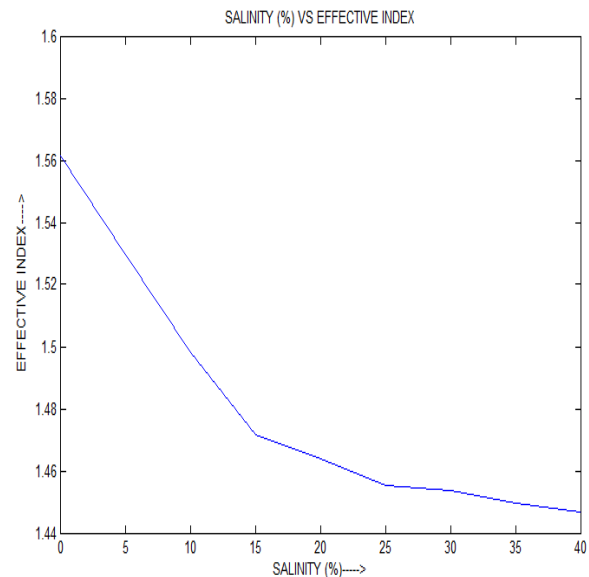


Figure 3: Salinity (%) against Effective Index

V. CONCLUSION

The slab waveguide sensor is designed for salinity measurement. The designed sensor is very sensitive even to the smallest change in refractive index, thus making it sensitive to change in the salinity percentage of the water. The photonic crystal core in the slab waveguide structure make is easier to fabricate and its compatibility with the optical cable enables it to create network in underwater environment.

REFERENCES

1. 'Salinity Meters – Regular Maintenance Tips', AG1392, Published: November 2009
2. 'Photonic crystal based sensor for sensing the salinity of Seawater', S. Robinson and R. Nakkeeran, IEEE International Conference on Advances in Engineering, Science and Management (ICAESM-2012), March 30-31, 2012
3. John D. Joannopoulos, Steven G. Johnson, Robert D. Meade, 'Photonic crystals modeling the flow of light', 2nd ed. 2008.
4. J.-F. Dong, J. Li, and F.-Q. Yang 'Guided modes in the four layer slab wave-guide containing Chiral Nihility Core' Progress In Electromagnetics Research, Vol. 112, 241{255, 2011.
5. <http://ab-initio.mit.edu/MEEP/Tutorial>
6. 'Two-Dimensional Photonic Crystal', by Susumu Noda et al. US patent number US7853111B2, 2010
7. Chapter 26, 'Optical Integrated Circuits', by Hiroshi Nishihara, Masamitsu Haruna, and Toshiaki Suhara.



Effective Code Coverage Test Suite Generation For Java Code

^[1]S.Narayanan, ^[2]T. Nandhinie

^[1]Faculty, ^[2]Student Department of CSE, Velammal Engineering College

^[1]prahladhan@gmail.com, ^[2]nandhiniet@gmail.com

Abstract ---- Software testing plays vital role in the software development process which widely uses validation approach in software industry by testers and developers. Innovated testing is needed to perform testing as whole and unit testing in a particular with minimum effort and time. Unit testing is mostly done by the developer to find the defects in the functionality of the products which illustrate the quality of it. Thus there is need in reducing the unit testing time by automating and optimizing the process. As effectiveness of testing highly depends on the test cases designed. Test cases can be generated automatically by inspecting the code either at the source level or at the intermediate level. Test suite which is the error prone and tedious. Thus a novel tool which generate test cases by traversing the code aim in achieving 100% coverage using a control flow method and Artificial Bee colony algorithm. Which then produce a effective and efficient coverage based test cases achieving the decision/branch coverage criteria.

Key terms: Software Testing, Coverage, Test Cases, Unit Testing, Artificial Bee colony Algorithm.

I. INTRODUCTION

Testing plays a very important phase in the software development process. Where the quality of end result depends on the large extends in testing. There are more than 50% of the software development organisation spend large portion of their budget in testing related activities. In which testing is illustrated as the process of exercising or evaluating a system or system components by manual or automated means to verify that it satisfies specified requirements. Are to say in different way testing is the process of identifying the difference between the expected and actual results. If the software fails from the expected outcome the testing efforts is to generate test cases to find that error. Here, test case is designed with the detailed internal functionality of the software with the external behaviour to incur the efficacy of the testing. Where test case is the main important data to elaborate the overall program expected outcomes; usage with common scenario Good test case will disclose possible defects with results in higher quality of testing process. White box testing which always focuses on the inner structure where always tester need to know about the knowledge of structure to design test case.

Existing test case design methods can be categorized into black-box testing and white-box testing. Black-box test cases are determined from the specification of the program under test and white-box test cases are derived from the internal structure of the software.

A test suite is a set of several test cases for a component or system under test, where the post condition of one test is often used as the precondition for the next one. The test suite optimization process involves generation of effective test cases in a test suite that can cover the given SUT within less time.

II. EXISTING SYSTEM

2.1 Meta Heuistics Search Techniques:

The use of meta heuristics search based techniques [2] used to automate the test data generation in various area such as black box, white box, grey box and non-functional area where the search based techniques are used in wide business application to detect, evaluate and find the key over the fields. To perform evolutionary testing, the task of test case design is transformed into an optimization problem and it can be solved with meta-heuristic search techniques. The search space is represented by the input domain of the system under test. Also the automation helps in saving of money and time and also the increase the quality of the products. All the application of the evolutionary techniques [2] is listed with the applied area of the Objective function. They are used in wide area of business application [9] for the improvement of testing. The MHS techniques used are hill climbing, evolutionary algorithms or simulated annealing.

Hill Climbing: hill climbing [2] is used to improve the single solution. The improvement in each step of better solution is climbing of hill by it local search rather than globally thus it also called as local search algorithm. There are two improvements in climbing:

Landscape which maximizes the objective function and steepest account which evaluate all the neighbours and the greatest improvement is taken as the current solution.

2.1.2 Evolutionary Algorithm

Genetic algorithm [2] is a search based technique which gives the optimal solution to the optimization problem. This is also a Meta heuristic which mimics the process of general evolution of selection, recombination and crossover. Larger classes of unit testing part use this evolution to find the

generation of each population. A population of candidate solution with a set of properties is determined for each solution. The population are generated randomly that is in iterative process where population occur in each iteration is called generation. For each generation fitness of individual in population is evaluated.

To be more precise a typical basic GA requires three basic components to be defined –

- a genetic representation of the solution,
- a fitness function to evaluate the candidate solutions and
- creation of new population.

2.2 Test Data Generation:

Test data generation [3] has the goal to provide input values that will traverse the paths received from the selector.

2.2.1 Random Test Data Generation

The random inputs are generated until we determine a actual inputs to be found out of it. The generation of the test data which fails due to random input and does not satisfy the requirement because of the requirements which is to be tested are not integrated. The various disadvantages of this method are such as it is appropriate only for simple and small programs, many sets of values may lead to the same visible behaviour and are thus redundant and the probability of selecting particular inputs that cause buggy behaviour may be enormously small. [3]

2.2.2 Dynamic And Static Test Data Generation:

Dynamic test-data generation technique collects information during the execution of the program and it determines which test cases come closest to satisfying the requirement. Static method generates test cases without execution of the program. It considers several constraints based on the input variables of the program under test. Instead of using variable substitution run the program with some selected possible random input. Consequently, values of variables are known at any time of the execution. By monitoring the program how the system can determine if the intended path was taken. If not, it backtracks to the node where the how took the wrong direction.

Using different kinds of search methods they can be altered by manipulating the input in a way that the intended branch is taken. This technique is quite expensive. It can require much iteration before a suitable input is found.[3]

Actual execution also suffers from the speed of execution for the program to analyze. Besides, to monitor the program flow code is instrumented, i.e. to put probes in the program to ascertain path traversal.

2.3 Symbolic Test Case Generation

Symbolic test data generation techniques assign symbolic values to the variables and create algebraic expressions for the several constraints in the program. A constraints solver is used to find a solution for these expressions that satisfies a test requirement. This technique cannot determine which symbolic values of the potential values will be used. The constraint solvers cannot produce floating point constraints

and hence floating point inputs cannot be found. Unit testing of classes [1] are analyse using genetic algorithm which is defines one goal at a time. The test cases are represented using individual chromosomes which consider the information of creating objects, state problem and invoking the methods. Chromosomes convert the order of statement with respect to the inputs parameter.

The possible step is to be followed to apply in each methods of class under test in different execution condition

1. Creating object for constructors.
2. The object is used to invoke the methods to work orderly.
3. The current test method is invoked.
4. Tested object which ends in state are compared to result of the test cases.

This initial method is used in testing to generate test cases at object under test. To minimize the procedure greedy algorithm is used by sequence selection of test case until it reaches the targeted coverage level.

Genetic algorithm examine all test case generation tools with improvement in the methods and fitness function to work more efficient then the other with enhancement in the feature with day to day technology.

To minimize the procedure of test case greedy algorithm [6] is used by sequence selection of test case until it reaches the targeted coverage level. There are two condemnatory choices in algorithm in : a) Fitness function for each test case is measured. b) Mutation operators. They are [1] is applied to some classes of the standard java library this up to 15 classes. As to generate test case we need to cover each statement of code which is only applicable manually rather than automate generation.

Here the test case generation using symbolic execution to solve the expression of the problem rather than the actual outcomes. In which the constraint solver cannot provide the floating point of the values.

24 Test Optimization

The process of generating test cases can be seen as a search or optimization process: there are possibly hundreds of thousands of test cases that could be generated for a particular SUT and from this pool we need to select, systematically and at a practical cost, those that comply to certain coverage criteria and are expected to be fault revealing. Hence, we can reformulate the generation of test cases as a search that aims at finding the optimal set of test cases from the space of all possible test cases. When software testing problems are reformulated into search problems, the resulting search spaces are usually very complex, especially for realistic SUT. The methods used to optimize the test suite are

A) Genetic Algorithm :

To evolve test suites [5] that optimize the chosen coverage criterion, we use a search algorithm, namely a Genetic Algorithm (GA). In this section, we describe the applied GA, the representation, genetic operations, and the fitness function.

Initially a random population, evolution is performed until a solution is found that fulfills the coverage criterion, or the allocated resources (e.g., time, number of fitness evaluations) have been used up. In each iteration of the evolution, a new generation is created and initialized with the best individuals of the last generation. Then, the new generation is filled up with individuals produced by rank selection, crossover, and mutation. Either the offspring or the parents are added to the new generation, depending on fitness and length constraints. The evosuite [5] compare the approach “entire test suite” to “one target at the time”. GA gives priority to the achieved coverage, with the secondary goal of minimizing the length. The performance is measured, where it yields two problems: (1) in practical contexts, we might not want a much larger test suite if the achieved coverage is only slightly higher, and (2) this performance measure does not take into account how difficult it will be to manually evaluate the test cases for writing asserts statements.

III. ARTIFICIAL BEE COLONY ALGORITHM

Artificial bee colony algorithm is motivated from the intelligent food foraging behaviour of honey bee insects. Honey bee swarm is one of the most intelligent swarms existing nature, which follows collective intelligent method, while searching the food. The honey bee swarms has many qualities like bees can communicate the information and take decision based on that. According to the change in the environment, the swarm updates itself, assign the tasks dynamically and moves further by social learning and teaching. The intelligent behaviour of bees motivates researcher to simulate above foraging behaviour of the bee swarm. The search process of ABC follows three major steps:

- Send the employed bee to a food source and calculate the nectar quality.
- Onlooker bees select the food source after gathering information from the employed bees and calculate the nectar quality.
- Determine the scout bees and employ them onto possible food source.
- The output it gives is the best solution it so far gathered is memorized.

IV. IMPLEMENTATION

The proposed system develop a tool for effective test suite generation which takes the control flow graph as a input and generate the efficient test cases for various variable using Artificial Bee colony (ABC) algorithm. The architecture of the proposed work is shown in fig 3.1. The control flow graph generator takes the source code as the input and the code is parser using Abstract Syntax Tree to indicate the predicate which is used to generate the test cases for the test methods. Fig

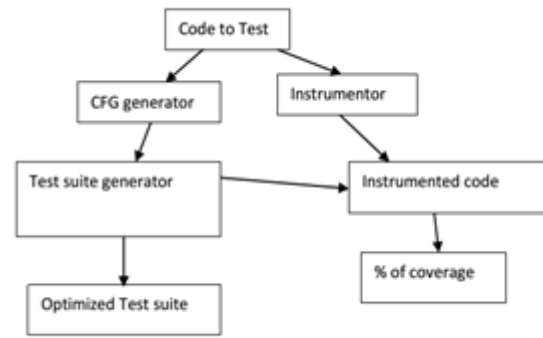


Fig3.

Modules:

The various steps in automation of framework in generating the effective and optimized test suite by following steps:

1. Taking the coding as the input CFG generator generates CFG Graph.
2. By analyzing the CFG the information regarding the predicate are extracted.
3. The test case is generated and by covering of each condition (expression) for the input domain of the variable.
4. The generated test cases are applied to instrument code to check the coverage.
5. The best test cases form an effective test suite.
6. Then junit framework is designed to structure the test suite generated to test run.

1. Code Parser and control flow :

Taking the source code as a input parsing the code and generating the control flow graph helps to determine the flows of code i.e., the path coverage and branch coverage/decision coverage.

2. Test case generation:

- By extracting the information from CFG and from the code the each test case are collected individually.
3. Efficient test suite: The generated test cases are gathered together to form a best test case by checking the coverage from the instrumentor code.
 4. Result analysis: The test suite are structured in a Junit Framework to further test run to find the code coverage of the all generated tests with the inside the code.

Result

These are the few snap shots for the implemented of efficient test suite



● ● ●

- [1] P. Tonella, "Evolutionary Testing of Classes," Proc. ACM SIGSOFT Int'l Symp. Software Testing and Analysis, pp. 119-128, 2004..
- [2] P. McMinn, "Search-Based Software Test Data Generation: A Survey," Software Testing, Verification and Reliability, vol. 14, no. 2, pp. 105-156, 2004.
- [3] Edvardson, J. 1999. "A Survey on Automatic Test data generation", In proceedings of the second conference on computer science and engineering Vol.2, No.1, pp.343-351.
- [4] M. Harman, S.G. Kim, K. Lakhotia, P. McMinn, and S. Yoo, "Optimizing for the Number of Tests Generated in Search Based Test Data Generation with an Application to the Oracle Cost Problem," Proc. Third Int'l Conf. Software Testing, Verification, and Validation Workshops, 2010
- [5] G. Fraser and A. Arcuri, "Evolutionary Generation of Whole Test Suites," Proc. 11th Int'l Conf. Quality Software, pp. 31-40, 2011.
- [6] Huaizhong Li et.al., "Software Test Data Generation using Ant Colony Optimization", Transactions on Engineering, Computing and Technology, ISSN 1305-5313, 2004.
- [7] B. Baudry, F. Fleurey, J.-M. Je'ze'quel, and Y. Le Traon, "Automatic Test Cases Optimization: A Bacteriologic Algorithm," IEEE Software, vol. 22, no. 2, pp. 76-82, Mar./Apr. 2005
- [8] D.Karaboga "An idea based on honey bee swarm for numerical optimization" Techn Rep.TR06,Erciyes Univ. Press,Erciyes,2005

Pattern Recognition Using Video Surveillance for Wildlife Applications

^[1]Meghana Badrinath N, ^[2]Nikhil Bharat, ^[3]Madhumathi S, ^[4]Kariyappa B.S.

^{[1][2][3]}Department of Electronics & Communication, RV College of Engineering, Bangalore, India

^[4]Professor, Department of Electronics & Communication, RV College of Engineering, Bangalore, India

^[1]meghana.badrinath@gmail.com, ^[2]bharat.nikhil@gmail.com, ^[3]madhu.1992@yahoo.com,

^[4]kariyappabs@rvce.edu.in

Abstract— Rapid increase in human population and their encroachment into forest areas have posed several threats to human life and their livelihood. This has subsequently led to a demand for real time surveillance systems that detect the entry of these animals and notify the concerned authorities. We propose a robust architecture that uses motion detection to isolate the potential targets in a visual scene. The target selection mechanism is based on a simple scheme for detecting moving objects. In addition, a pattern recognition module will analyze potential targets using Histogram of Oriented Gradients (HOG) algorithm, in order to distinguish the harmful animals from innocuous ones. Compared to traditional algorithms, HOG offers significantly higher accuracy. Further, the system also includes a GSM and GPS module to apprise the forest department about the type and location of the detected animal respectively. Through software and hardware debugging and actual estimation, our system was found to reach the expected goal.

Index Terms—Histogram of Oriented Gradients(HOG), Motion Detection, Pattern Recognition, Support Vector Machine (SVM)

I. INTRODUCTION

Due to the limitations of current wildlife monitoring technologies, the behaviour of free ranging animals, remains largely unknown. Deficit of efficient real time surveillance systems limits the ability to determine the entry of an animal in order to take suitable protective measures. Hence, there is a need to develop a robust method for tracking animals using state of the art imaging techniques.

Processing large number of images, for identification of animals continues to remain a challenge. At present, all camera-based studies of wildlife use a manual approach where researchers examine each photograph to identify the species in the frame. For studies collecting several photographs, this is a daunting task.

Hence, there is a need for a system which not only captures the image of trespassing animals but also classifies them as harmful. This system should further duly notify the concerned authorities.

II. RELATED WORK

M.A.H.B. Azhar, S. Hoque, F. Deravi, in their work of tracking of individual animals using distinctive skin patterns on the belly, for population estimation of The Great Crested Newt, specify the identification of individual animals by segmenting the Region of Interest (ROI). This method was found to be particularly useful for the identification of animals with skin patterns, which when detected can automatically be utilised to classify the animal [1].

Thiago C. Silva, Thiago H. Cupertino, and Liang Zhao proposed a data classification technique which combines both low level and high level learning. Low level learning,

classifies data instances by their physical features. On the other hand, high level learning measures the compliance to the pattern formation. The method proposed in this paper is particularly useful in ensuring that the technique used for pattern classification is reliable and offers a good hit rate [2].

Angel Noe Martinez-Gonzalez and Victor Ayala-Ramirez introduced a method of using neural networks to develop a face detection system which is capable of operating in real time. The system used human skin colour properties to perform a face search, these properties are then detected on a pixel by pixel basis [3].

Narges Ghaedi Bardeh and Maziar Palhang presented a bag-of-features model for human detection. Visual words described by HOG are clustered using K-means algorithm. This is followed by a Support Vector Machine (SVM) as their classifier [4].

III. MOTIVATION

In recent times, there has been a severe loss of animal habitat due to industrialization and explosion of human population. There is, hence, very little distinction between forest and urban areas, forcing the animals into villages. Incidents of man-animal conflict are reported from different States and Union Territories. The World Wildlife Fund estimated that only about 3,200 tigers are left in the world. At the same time, the number of tiger attacks is up 30 percent over the past decade. Also in India, wild elephants probably kill far more people than tigers, leopards or lions. But, surprisingly, human conflict involving leopard draws great amount of public attention compared to other animals. The Government is giving highest priority to mitigate the problem. Animals like elephant, tiger, leopard, wild dog, wild boar, bear, etc. are major animals involved in human-animal conflict in India.

IV. METHODOLOGY

Computer-assisted species recognition on images captured by a camera could make the task of recognising more efficient, and reduce, if not remove, the amount of manual work involved in the process. However, in comparison with the typical video from surveillance of building and street views, camera trap of animals amidst vegetation are more difficult to incorporate into image analysis routines because of low frame rates, background clutter, poor illumination, image occlusion, and complex pose of the animals.

Camera-based studies of wildlife require using image analysis to identify individual animals based on their skin texture and patterns (if any), body contour and presence of explicit features like horns, trunks and tails. Identification of individual animal species is a non-trivial task. The basic steps involved in the detection of an animal and subsequent classification would include motion detection and pattern recognition is illustrated in fig1.

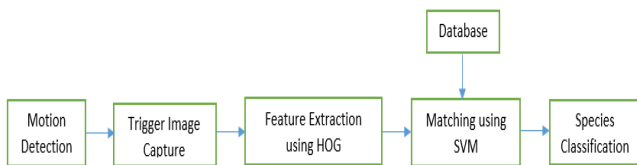


Fig 1. Block Diagram of animal recognition system

A. Image Acquisition

Particular to the field of wildlife imaging is the requirement of efficient memory utilisation. To facilitate this, the module enables the user to identify the region to be concentrated on. This eventually eliminates the possibility of false alarms that maybe triggered due to irrelevant movement.

The proposed system triggers the sensors to capture an image only when it detects motion. The motion detection algorithm needs to be insensitive not only to movement of surrounding vegetation but also variations in climatic conditions. In order to achieve the aforementioned objective the camera continuously captures images of low resolution. Only when sufficient movement is detected, a high resolution image is captured. Consequently the low resolution images are erased from memory, retaining only those images that carry substantial amount of relevant information.

Frame differencing is subsequently carried out to find the number of varying pixels between two consecutive frames. If the number of pixels with different RGB values is beyond the set threshold, it is an indicator of motion. This will trigger the camera to take an image which is then passed on to the pattern recognition module

B. Pattern Recognition

The human mind learns to differentiate between animal species through experience. This is not as easy in a computer since it will have to be trained to do the task. An extensive database of all the animals consisting of labelled images will have to be created. This includes positive and negative images which provide the computer the ability to differentiate between the animal species and be capable of taking further action.

For our purpose, we make use of Histogram of Oriented Gradients (HOG) algorithm for animal detection. HOG is popularly used for human face detection. Although performance of HOG is significantly better than other face detection algorithms, it is a computationally intensive process since the dimensions of the descriptor vectors are very large. Despite these shortcomings, HOG was chosen to be the suitable algorithm because like human faces, animal faces also have fixed inter-class structure. This ensures a good hit rate that is vital for reliable performance of the system.

The steps involved are as follows-

1. The first step in this algorithm would be to normalize the colour and gamma values. In order to perform this, the following derivative mask is used for filtering -

$$H = [-1 \ 0 \ 1]^T$$

2. The image is then divided into a number of cells. In order to make the algorithm more robust, the cells are grouped into blocks.

3. A user defined window is then applied to the image to calculate the gradients of each pixel.

4. The presence of blocks can account for changes in illumination and contrast, by locally normalizing the gradient strengths.

5. The HOG descriptor is the vector of the components of the normalized cell histograms from all of the block regions.

6. After calculating gradients for all pixels in each cell of the image, they will be quantized into a user defined number of bins.

For optimum results, the components are organized into 9 bins with a range of 20 degrees per bin.

7. The next step is to normalize each of the blocks. This step finally yields a normalized column vector.

8. The final step involves feeding the extracted features to a classifier. For the case of pattern recognition, Support Vector Machine (SVM) classifier is used.

SVM classifier is a binary classifier which fits an optimal hyper plane as a decision boundary. Once trained on images containing some particular object, the SVM classifier can make decisions regarding the presence of an animal in a group of test images.

C. Communication Module

After a reliable decision about the animal species has been made by the preceding module, it is important to convey the same to the relevant authorities. This ensures that they can take suitable precautions to prevent the inadvertent consequences caused by animal entry. For this purpose a GSM unit can be utilized. Since the systems are proposed to be installed in forest-village boundaries, it is assumed that mobile network is available. A GPS module helps in conveying precise information about the location of animal trespass.

In the absence of mobile network, an alternate means of communication such as Wi-Fi can also be utilized.

Fig 2. Demonstrates the complete prototype for animal detection and tracking. The presence of an actuation module in the system facilitates tranquilization of the animal based on its species in order to avert potential damage.

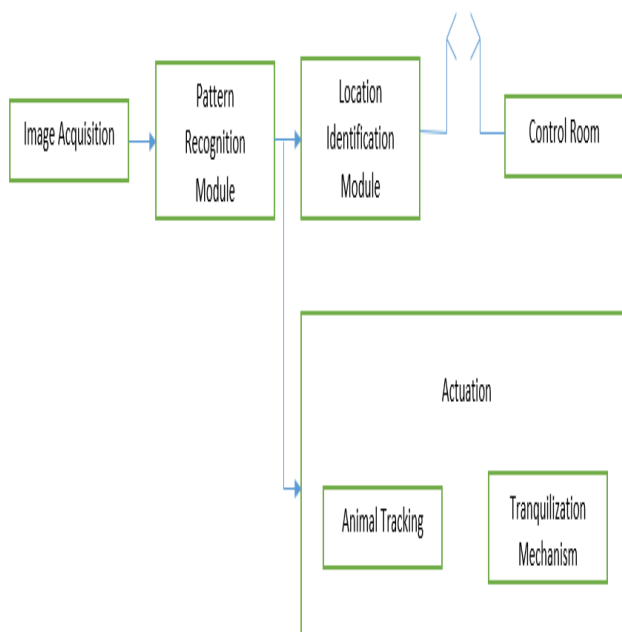


Fig 2. Block Diagram of Wildlife Monitoring and Actuating System

V. RESULTS

For the purpose of simulation, a database of harmful animals and harmless animals were created. 263 images of harmful animals were taken, comprising of tigers, lions, elephants, leopards and cheetahs. The harmless animals taken for our study included different types of deer, zebras, giraffes and all kinds of farm animals. This set included 450 images. Fig. 3 and 4 demonstrate a sample set of the harmful and harmless animals respectively.

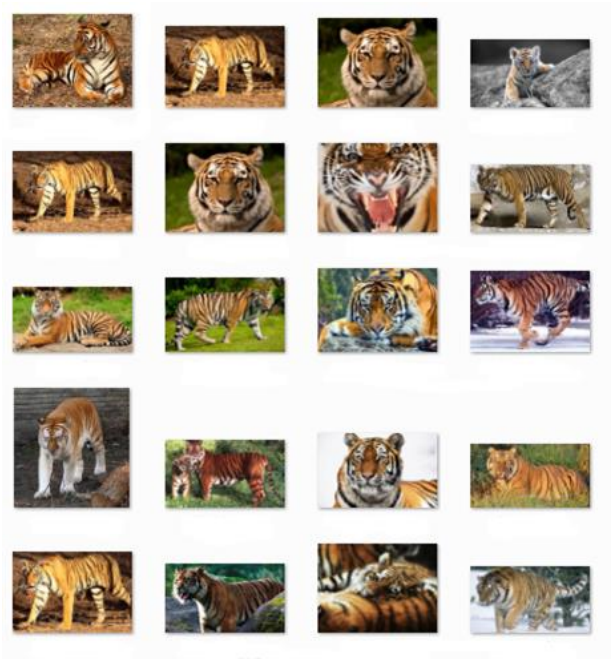


Fig 3. Training set - Harmful Animals(Tigers)

These training images were fed into a multilayer neural network. HOG algorithm was used for each of the training images, resulting in an 81 X 1 column vector.

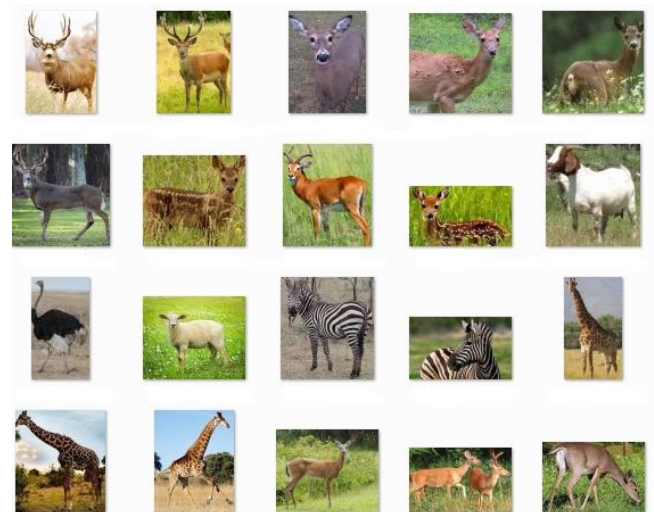


Fig 4. Training set - Harmless animals

For the purpose of classification, HOG features of each individual animal is extracted. This is in turn utilized by the SVM module.

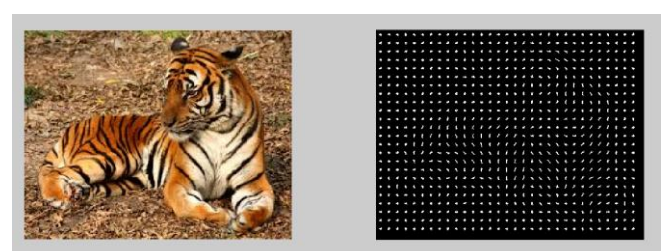


Fig 5. HOG features of tiger image

Subsequently SVM based training was performed on all the training images to yield a training matrix. Binary labels were assigned to each of the training matrices. This was followed by SVM based classification. Ten testing images are shown in fig 6. The classification algorithm was clearly able to detect and segment the tiger as illustrated.



Fig 6. Simulation Results for tiger identification

Since SVM is a binary classifier, successive classification was performed in case the animal was categorized as harmful. The final stage in our pattern detection approach clearly detected and identified the type of animal as demonstrated in the flowchart in fig 7.

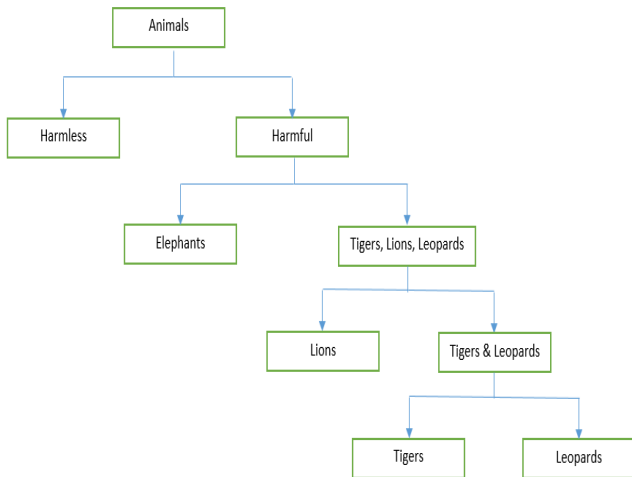


Fig 7. Animal Classification Flowchart

VI. CONCLUSION

The paper outlines one of the methods to safeguard human habitation by enabling the relevant personnel to be more responsive to animal intrusion through the intelligent video surveillance system. The simulation results indicate that the adopted Histogram of Oriented Gradients algorithm, for pattern recognition of animals, is suitable for the intended

application. A peripheral device can be incorporated into the system, which utilizes the data obtained from the pattern recognition module, to enable on-site tranquilization of the intruding animal.

VII. ACKNOWLEDGMENT

We would like to thank Mr. T Vasu, Director technical, QED Agro Systems Private Limited, for his technical assistance and constant encouragement.

We also express our gratitude to The Department of Electronics & Communication for providing us the necessary support and environment to work on this endeavour.

REFERENCES

- [1] M.A.H.B. Azhar, S. Hoque, F. Deravi, "Automatic Identification of Wildlife using Local Binary Patterns", *IET Conference, Image Processing (IPR)*, 2012.
- [2] Thiago C. Silva, Thiago H. Cupertino, and Liang Zhao, "High Level Classification for Pattern Recognition," 24th SIBGRAPI Conference on Graphics, Patterns and Images, 2011.
- [3] Angel Noe Martinez-Gonzalez and Victor Ayala-Ramirez, "Real Time Face Detection Using Neural Networks," *10th Mexican International Conference on Artificial Intelligence*, 2011
- [4] Narges Ghaedi Bardeh and Maziar Palhang, "New Approach for Human Detection in Images Using Histograms of Oriented Gradient," *21st Iranian Conference on Electrical Engineering*, 2013.
- [5] Sorin M. Jacob and Alfons H. Salden, "Attention and Anticipation in Complex Scene Analysis - An Application to Video Surveillance," *IEEE International Conference on Systems, Man and Cybernetics*, 2004.
- [6] Tilo Burghardt and Janko Calic, "Real-time Face Detection and Tracking of Animals," *8th Seminar on Neural Network Applications in Electrical Engineering, NEUREL*, 2006.
- [7] D. Tweed and A. Calway, "Tracking multiple animals in wildlife footage," *16th International Conference on Pattern Recognition*, 2:24 27, 2002.
- [8] Bogdan Kwolek, "Multiple Views Based Human Motion Tracking in Surveillance Videos," *8th IEEE International Conference on Advanced Video and Signal-Based Surveillance*, 2011.
- [9] Chaoyang Zhang, Zhaoxian Zhou, Hua Sun, and Fan Dong, "Comparison of Three Face Recognition Algorithms", *International Conference on Systems and Informatics*, 2012.
- [10] Samantha D.F. Hilado, Elmer P. Dadios, Laurence A. Gan Lim,

Edwin Sybingco, Isidro V. Marfori, Alvin Y. Chua " Vision Based Pedestrian Detection Using Histogram of Oriented Gradients, Adaboost & Linear Support Vector Machines," *IEEE Region 10 Conference*, 2012.



Development of an FPGA-Based SPWM Generator for High Switching Frequency DC/DC Buck-Boost converters

^[1]S.L.Binu,^[2] Mr.M.Afsar ali

^[1]VLSI Design, S.K.R.Engineering college Chennai,^[2] ECE Dept S.K.R.Engineering college Chennai
^[1]shreejitha.jiotha@gmail.com,^[2]contactafsar@gmail.com

Abstract—The digital implementations of Sinusoidal Pulse Width Modulation (SPWM) generators have dominated over their counterparts based on analog circuits. In this paper, an FPGA based SPWM generator is presented, which is capable to operate at switching frequencies up to 1 MHz (requiring FPGA operation at 100–160 MHz), thus it is capable to support the high switching frequency requirements of modern single-phase dc/dc buck-boost power converters. The proposed design occupies a small fraction of a medium-sized FPGA and, thus, can be incorporated in larger designs. Additionally, it has a flexible architecture that can be tuned to a variety of dc to dc buck- boost converter applications. The post layout simulation and experimental results confirm that compared to the past-proposed SPWM generation designs, the SPWM generator presented in this paper exhibits much faster switching frequency, lower power consumption, and higher accuracy of generating the desired SPWM waveform.

Index Terms—DC/DC buck-boost converter, field programmable gate array (FPGA), high frequency, sinusoidal pulse width modulation

I. INTRODUCTION

The dc/dc converters (inverters) are the major power electronic conversion units in renewable energy production, motor drive, and uninterruptible power supply applications. A simplified block diagram of a single-phase, full bridge dc/dc power converter (inverter) is depicted in Fig. 1. The Sinusoidal Pulse Width Modulation (SPWM) technique is widely employed in order to adjust the dc/dc inverter output voltage amplitude and frequency to the desired value. In the existing method they used SPWM generator which used in for high switching frequency used in dc/ac buck-boost converter. In this case, the power converter switches (e.g., MOSFETs, IGBTs, etc.) are set to the ON or OFF state according to the result of the comparison between a high-frequency, constant-amplitude triangular wave (carrier) with two low-frequency (e.g., 50 Hz) reference sine waves of adjustable amplitude and/or frequency. The **buck-boost converter** is a type of DC-to-DC converter that has an output voltage magnitude that is either greater than or less than the input voltage magnitude.

Two different topologies are called *buck-boost converter*. Both of them can produce a range of output voltages, from an output voltage much larger (in absolute magnitude) than the input voltage, down to almost zero.

In the unipolar SPWM technique illustrated in Fig. 2, the generated pulses are either positive or **negative during each half period of the SPWM wave**. The high-frequency harmonics of the generated SPWM signal, V_s pwm in Fig. 2,

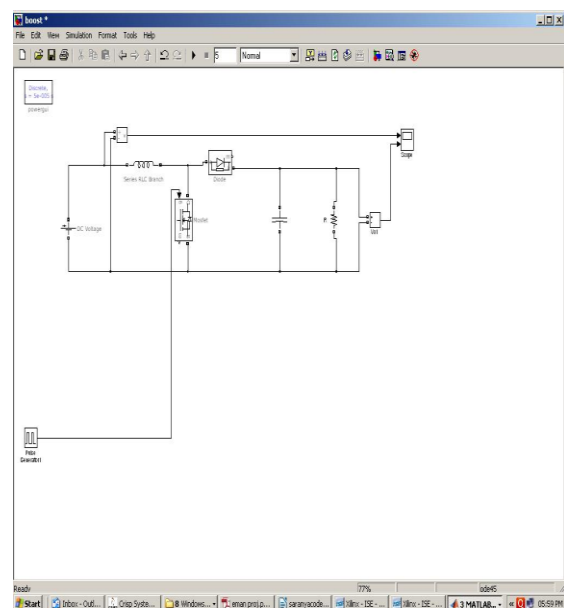


Fig. 1. Block diagram of a single-phase, full-bridge dc/dc power converter.

Using FPGAs for the development of the dc/c inverter control logic has widely emerged during the last years since they are considered as a powerful and cost-effective solution. Compared to the microcontroller and DSP-integrated circuits, FPGAs have the advantage of flexibility in case of changes and they enable the reduction of the execution time of the dc/dc inverter control algorithm due to their capability to integrate

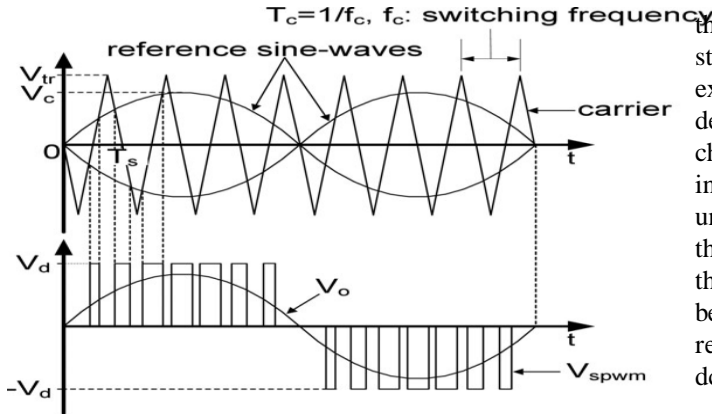


Fig. 2. Unipolar SPWM technique.

digital hardware with high speed and parallel processing features. In the FPGA-based SPWM generation units presented in the triangular wave is implemented in the form of an up-down counter. The corresponding samples are stored in digital format in a lookup table (LUT) implemented in the FPGA internal memory. The CORDIC algorithm has also been applied in for the development of an integrated circuit performing the generation of a 5-kHz SPWM wave using 0.18- μm CMOS technology. In , an LUT is used to store the reference sine-wave digital values corresponding to the time instants of the peaks and nadirs of the triangular wave. The width of each pulse is calculated using an equation based on the similarity of the triangles ABC and ADF depicted in Fig. 3(b). This design method has been validated in case of a 1-kHz switching frequency. A similar approach is also proposed in . In , the SPWM pulse train is produced by comparing the sinusoidal and triangular signals generated according to the direct digital synthesis (DDS) technique. The comparison is performed using a high-speed analog comparator. The DDS approach is also used in for the development of a digital SPWM generator chip using 0.35- μm CMOS technology. The maximum clock frequency of this chip is 50 MHz. In , the SPWM unit is composed of a DSP chip accomplishing the calculation of the widths of the individual pulses comprising the SPWM wave, which communicates through a parallel port with an FPGA-based unit producing the SPWM control signals. The regular-sampled PWM technique presented in , targets to reduce the amount of computation time required in order to facilitate the generation of higher switching frequencies online and in real time. In this technique, the pulse width is calculated once and used over N consecutive switching edges of the SPWM wave pulses. Then, a new sample of the reference sine wave is acquired. Thus, the sampling frequency f_s is reduced by an integer factor of N , resulting in the following relationship with the corresponding carrier frequency f_c : $f_s = f_c/N$. (2) Consequently, the number of calculations required to produce the complete SPWM waveform is N times less than in the conventional SPWM generation methods. In this paper, an FPGA-based SPWM generator is presented, which is capable to operate at switching frequencies up to 1 MHz; thus, it is capable to support the high switching frequency requirements of modern single-phase dc/dc power converters. Compared to the past-proposed SPWM generators in the proposed architecture

the values of both the reference sine and triangular waves are stored in the FPGA device Block RAMs (BRAMs) in order to exploit their one-clock cycle access time. The proposed design exhibits architectural flexibility features, enabling the change of the SPWM switching frequency and modulation index either internally, or externally. The proposed SPWM unit has been implemented in a single chip in order to enable the reduction of the complexity, cost, and development time of the dc/dc inverter control unit. The proposed SPWM unit has been implemented in a single chip in order to enable the reduction of the complexity, cost, and development time of the dc/dc inverter control unit.

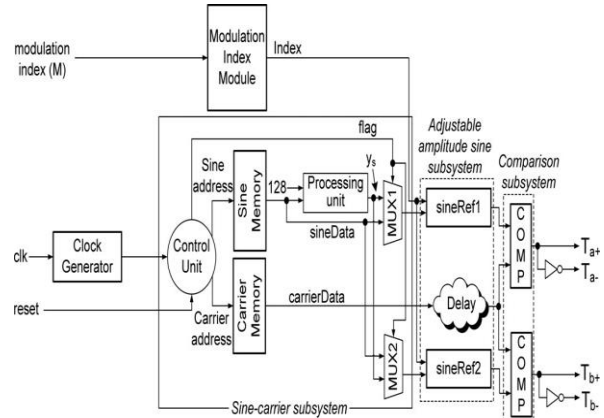


Fig. 3. Architecture of the proposed SPWM generation unit.

..And the carry select adder is used in the processing unit instead of the existing system.

The architecture of the proposed FPGA-based SPWM generator is analyzed in Section II, and the simulation and experimental results are presented in Section III. Finally, the performance of the FPGA generator presented in this paper is compared to that of the past-proposed systems, and the corresponding results are analyzed in Section IV.

II. PROPOSED SPWM GENERATOR

The architecture of the proposed SPWM generation unit is presented in Fig. 3. The system inputs are the modulation index of the output SPWM wave M in single precision floating point arithmetic ranging from 0 to 1, as well as the “clock” and “reset” signals. The architecture of the proposed system has been built using 8-bit fixed-point arithmetic and it consists of five subsystems, which implement the SPWM generation algorithm. And we use carry select adder in the processing unit instead of the existing system.

A. Clock Generator Subsystem

The “Clock generator” subsystem takes as input the FPGA input clock and produces a new clock signal used by the digital circuits of the proposed SPWM generator, such that the desired SPWM switching frequency f_c specified by the designer/user is generated. A two-state finite state machine (FSM) is initially used to set the input clock frequency f_{clk} to $f_{clk}/2$ and then a Digital Clock Manager module adapts this frequency to the

Desired value.

B. Modulation Index Subsystem

The “Modulation index” subsystem is used to convert the floating-point modulation index M , which is input in the proposed SPWM generation system ($M \in [0, 1]$) to the corresponding value in fixed-point arithmetic. Initially, the value of M is transformed into a new floating point value yM according to the following equation:

$$yM = M \cdot (2n-1 - 1) + 2n-1 \quad (3)$$

where n is the digital word length of the architecture. Increasing the value of n enables to control the modulation index of the generated SPWM wave with higher resolution, but also results in higher requirements for FPGA device resources. The floating point value produced is then converted into a fixed-point value ranging from 0 to 255, via a float-to-fixed point conversion unit, thus producing the “Index” output of the “Modulation index” subsystem depicted in Fig. 4.

C. Sine-Carrier Subsystem

The “Sine-Carrier” subsystem consists of the control unit, two BRAMs, which contain samples of the sinusoidal and triangular (i.e., carrier) waves and two multiplexers that produce the two constant-amplitude reference sine waves used for the production of the SPWM output signals. The BRAMs of the sine wave and carrier operate as LUTs. Both the sinusoidal and triangular waves are sampled and quantized with the same sampling frequency f_s using MATLAB (e.g., $f_s = 4, 8$ MHz, etc.). In order to minimize the utilization of the FPGA resources, only the values of the first quarter of the constant amplitude sine-wave period (i.e., during the time interval $0 - \pi/2$) are stored in the corresponding BRAM, while the values of the sine wave during the time interval $\pi/2 - 2\pi$ are calculated by mirroring and inverting the values of the first quarter. The BRAM of the carrier contains the values of a complete period of the reference triangular wave. Consecutive addresses of both memories (“Sine address” and “Carrier address,” respectively, in Fig. 4) are generated in every clock cycle by the control unit. The control unit also produces a “flag” signal, which is responsible for the retrieval of the sine-wave values during the time interval $\pi - 2\pi$ of the reference sine-wave period. The BRAM of the constant-amplitude sinusoidal wave is scanned up and down four times, since this memory contains only the values during the first quarter of the sinusoidal-wave period, as analyzed previously. The FSM generating the addresses of the sinusoidal and carrier memory pointers, “sineAddr” and “car Addr,” respectively. The first state of this FSM (i.e., “State 0”) contains all possible conditions of the memory address pointers. The value of the “flag” signal determines the up or down direction of consecutive accesses performed for retrieving the data stored in the BRAM memory of the reference sine wave. While “flag” is set to 0, the multiplexer “MUX1” outputs the data read from the constant-amplitude sinusoidal memory. Otherwise, “MUX1” outputs the values corresponding to the second half-cycle (i.e., during $\pi - 2\pi$) of the constant-amplitude sinusoidal wave (parameter “ys” in Fig. 4). These values are produced by the processing unit of

the “Sinecarrier subsystem” by converting the positive values stored in the sinusoidal memory to the corresponding negative values, according to the following equation: $ys = x - [(x - 2n-1) \times 2]$ (4) where x is the positive value stored in the BRAM of the sine wave. The multiplexer “MUX2” is used for the production of the second constant-amplitude reference sine wave, which operates with a 180° phase difference compared with the one analyzed above.

D. Adjustable Amplitude Sine Subsystem

The “Adjustable amplitude sine” subsystem takes as input the constant-amplitude reference sinusoidal values produced by the “Sine-Carrier” subsystem and generates a sinusoidal digital signal ya with an amplitude adjustable according to the value of the modulation index M which is an input in the proposed SPWM generation system.

E. Comparison Subsystem

The “Comparison” subsystem implements the comparison between the high-frequency constant-amplitude triangular wave (carrier) with the two low-frequency reference sine waves, using two comparators (“COMP” in Fig. 4). The control signals $Ta+$, $Ta-$, $Tb+$, and $Tb-$ of the single-phase dc/dc inverter power switches depicted in Fig. 1 are generated from the outputs of the corresponding comparators of this subsystem, thus forming the SPWM wave (V_{spwm} in Figs. 1 and 2) at the dc/dc inverter output terminals. The outputs of the comparators in the “Comparison” subsystem (i.e., control signals $Ta+$ and $Tb+$) are equal to one when the corresponding output of the “Adjustable amplitude sine” subsystem described in Section II-C is equal to or greater than the current digital value of the carrier signal. The DC/DC inverter control signals $Ta-$ and $Tb-$ are produced by inverting $Ta+$ and $Tb+$, respectively.

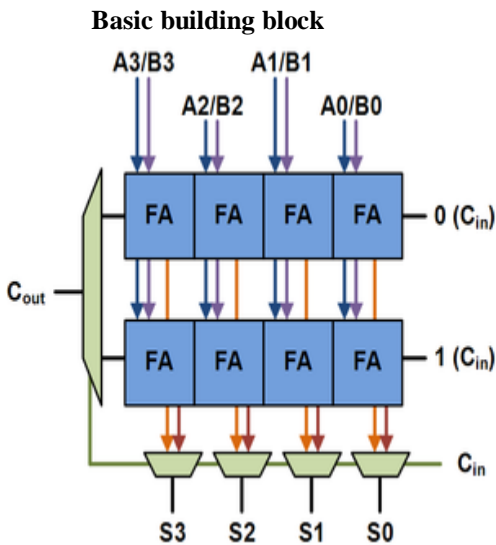
F. Processing unit

In this processing unit we use carry select adder instead of the existing system. In electronics, a **carry-select adder** is a particular way to implement an [adder](#), which is a logic element that computes the $(n+1)$ -bit sum of two n -bit numbers. The carry-select adder is simple but rather fast, having a gate level depth of $O(\sqrt{n})$.

The carry-select adder generally consists of two ripple carry adders and a multiplexer. Adding two n -bit numbers with a carry-select adder is done with two adders (therefore two ripple carry adders) in order to perform the calculation twice, one time with the assumption of the carry being zero and the other assuming one. After the two results are calculated, the correct sum, as well as the correct carry, is then selected with the multiplexer once the correct carry is known.

Above is the basic building block of a carry-select adder, where the block size is 4. Two 4-bit ripple carry adders are multiplexed together, where the resulting carry and sum bits are selected by the carry-in. Since one ripple carry adder assumes a carry-in of 0, and the other assumes a carry-in of 1,

selecting which adder had the correct assumption via the actual carry-in yields the desired result.



Uniform-sized adder

A 16-bit carry-select adder with a uniform block size of 4 can be created with three of these blocks and a 4-bit ripple carry adder. Since carry-in is known at the beginning of computation, a carry select block is not needed for the first four bits. The delay of this adder will be four full adder delays, plus three MUX delays.

Variable-sized adder

A 16-bit carry-select adder with variable size can be similarly created. Here we show an adder with block sizes of 2-2-3-4-5. This break-up is ideal when the full-adder delay is equal to the MUX delay, which is unlikely. The total delay is two full adder delays, and four mux delays. We try to make the delay through the two carry chains and the delay of the previous stage carry equal.

III. PERFORMANCE

A. System Validation by Simulation

The architecture presented in the previous section has been synthesized using the VHDL language and its correct operation has been verified at both low- and high-carrier frequency levels using the ModelSim 6.3f simulator. A low-carrier frequency has been used in this example only for discrimination of all SPWM pulses produced within a period of the reference sine wave and the observation of their width. As analyzed in Section II, the SPWM output is generated at the intersection of the sinusoidal and triangular waveforms at certain sampling instants. When the value of each sine wave is higher than the triangular wave value, the output pulse is set to logical "1," else it is set to logical "0."

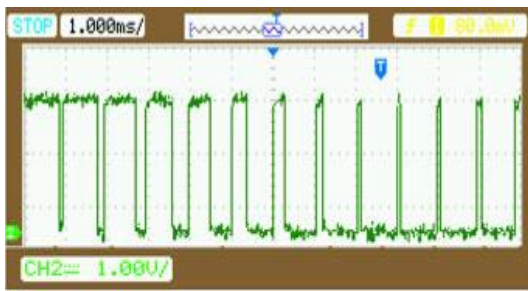
B. Experimental Results

A laboratory prototype of the proposed FPGA-based SPWM generation system (see Fig. 4) was implemented using the commercially available XILINX XUPV5-LX110T development board for downloading the implemented SPWM

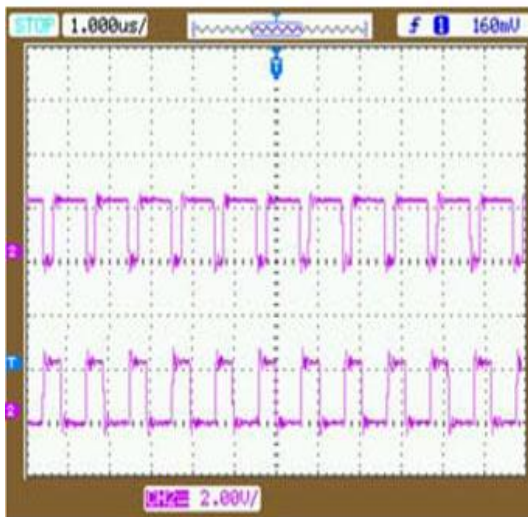
design, which contains the XC5VLX110T Virtex-5 FPGA device. The proposed SPWM generator is suitable for incorporation in single-phase dc/ac inverter applications and as an example, the experimental, oscilloscope measurements of the $Ta+$ SPWM control signal ($Ta-$, $Tb+$, and $Tb-$ exhibit similar patterns) in case that $f_c = 1$ kHz and $f_c = 1$ MHz, respectively, are illustrated in Fig. 8. Using a 1-MHz carrier frequency, results in 20 000 pulses spread over the 1/50 Hz time period of the $Ta+$ signal. Thus, in order to enable the visibility of the individual SPWM pulses, two different portions of this signal are illustrated separately in the upper and lower waveforms, respectively, which are plotted in Fig. 8. Then, a unity-gain differential amplifier was used in order to subtract the $Ta+$ and $Tb+$ control signals generated by the proposed SPWM generation system. This hardware-emulation process has the advantage of low cost, since building an actual power stage of a single-phase dc/dc inverter (including power switches, drivers, etc.) is avoided. Additionally, it enables to evaluate the performance of the proposed SPWM generator without being affected by non-idealities of an experimental prototype dc/dc power inverter (e.g., dead-time effect, power switch finite turn-on, and turn-off times, etc.), which depend on the exact type of the dc/ac inverter application comprising the proposed SPWM generator and deteriorate the quality of the generated SPWM signal. The minimization of the impact of such effects is performed during the design process of the dc/dc inverter; thus, the investigation of their impact on the quality of the SPWM output voltage of the dc/ac inverter is not within the scope of this paper. The hardware-emulation process described previously has been applied in order to experimentally evaluate the performance of both the new SPWM generator presented in this paper, as well as that of the past-proposed SPWM generation units. The corresponding experimental results are presented in the following paragraphs of this paper. The Fast Fourier Transforms (FFTs) of the experimentally measured SPWM output waveforms, which are produced by the hardware emulation process described previously, in case that the SPWM switching frequency f_c is 1 kHz and 1 MHz. It is observed that, as expected due to the attributes of the unipolar SPWM.

IV. CONCLUSION

The SPWM principle is widely used in dc/dc converters in energy conversion and motor drive applications. The past proposed SPWM generators have been designed to operate at low switching frequencies (i.e., 1–20 kHz), while their operation at higher switching frequencies had not been explored so far. In this paper, an FPGA-based SPWM generator has been presented, which is capable to operate at switching frequencies up to 1 MHz, thus it is able to support the high switching frequency requirements of modern single-phase dc/dc converters. The proposed design occupies a small fraction of a medium sized FPGA and, thus, can be incorporated in larger designs, while it has a flexible architecture can be adapted to a variety of single-phase dc/dc converter applications. Both post place and route simulation results and experimental verification results on actual



(a)



(b)

Fig. 4. Oscilloscope measurements of the $Ta+$ SPWM control signal:



(a) $f_c = 1$ kHz, $f_s = 4$ MHz, and $M = 0.9$ and (b) $f_c = 1$ MHz, $f_s = 32$ MHz, and $M = 0.5$.

hardware were presented, demonstrating the successful operation of the proposed SPWM generator at high switching frequencies.. The post layout simulation and experimental results confirm that the proposed SPWM generator exhibits much faster switching frequency, lower power consumption, and higher accuracy of generating the desired SPWM waveform.

REFERENCES

- [1] R. Teodorescu, M. Liserre, and P. Rodr'iguez, *Grid Converters for Photovoltaic and Wind Power Systems*, 1st ed. New York, NY, USA: Wiley, 2011.
- [2] N. D. Patel and U. K. Madawala, "A bit-stream-based PWM technique for sine-wave generation," *IEEE Trans. Ind. Electron.*, vol. 56, no. 7, pp. 2530–2539, Jul. 2009.

Study on Internal Curing of Concrete Using Admixtures

^[1]A.Sivaranjani, ^[2]M.Monica, ^[3]V.R.Subhashini, ^[4]S.Sareetha, ^[5]M.S.Kuttimarks, ^[6]Er.B.Sudhakar Senthil Vasan

^{[1],[2],[3],[4]}BE-Student, ^[5]Assistant Professor Department of Civil Engineering, Sree Sastha Institute of Engineering and Technology, Chennai-123, ^[6] Assistant Director, Concrete and Structures laboratory Highway Research Station, Chennai-25.

^[1]sivaranjaniavudaiyappan93@gmail.com, ^[5]kuttimarkskmpm@gmail.com

Abstract— This paper compares the compressive Strength of the concrete conventional curing process and Self curing process. Curing is a process to maintaining satisfactory moisture content and temperature in concrete in order to achieve the desired strength and hardness. A concept of self curing has been introduced in order to eliminate the water required for the curing process. Internal curing is mainly provided to absorb water from atmosphere to achieve better hydration of cement in the concrete. The self-curing materials are added to a dosage of about 0.5% by weight of cement as Natural fibres like Sisal and Polymeric agent like polyethylene glycol 400 (PEG400) has been used. The expected Compressive strength is achieved by means of self curing materials.

Index Terms—Internal curing, Natural fiber, Polymeric agents

I. INTRODUCTION

Concrete is a composite material composed of coarse granular material (the aggregate or filler) embedded in a hard matrix of material (the cement or binder) that fills the space among the aggregate particles and glues them together. Famous concrete structures include the Hoover Dam, the Panama Canal and the Roman Pantheon. The earliest large-scale users of concrete technology were the ancient Romans, and concrete was widely used in the Roman Empire. The Colosseum in Rome was built largely of concrete [5], and the concrete dome of the Pantheon is the world's largest. After the Roman Empire collapsed, use of concrete became rare until the technology was re-pioneered in the mid 18th century. Today, concrete is the most widely used man-made material (measured by tonnage).

1.1 Curing Of Concrete

Curing is described as a process of maintaining satisfactory moisture content and a favorable temperature in concrete during the period immediately following placement [1, 2], so that hydration of cement may continue until the desired properties are developed to a sufficient degree to the requirement of service. It has been recognized that the quality of concrete shows all round improvement with efficient un-interrupted curing. This process results in concrete with increased strength and decreased permeability. Curing is also a key player in mitigating cracks, which can severely affect durability [7]. Good curing can help mitigate the appearance of un-planned cracking. The duration and type of curing plays a big role in determining the required materials necessary to achieve the high level of quality. Conventionally, curing of concrete means creating

conditions such that water is not lost from the surface [5] i.e., curing is taken to happen 'from the outside to inside'.

As per **IS 456-2000**,

"Curing is the process of preventing the loss of moisture from the concrete."

The **ACI-308** Code states that "internal curing refers to the process by which the hydration of cement occurs because of the availability of additional internal water that is not part of the mixing Water."

1.2 Methods Of Curing

The different methods of curing available are as follows:

- ❖ Water curing
- ❖ Membrane curing
- ❖ Application of heat
- ❖ Miscellaneous

II. INTERNAL CURING

An internal curing concrete is provided to absorb the water from atmosphere from air to achieve better hydration of cement in concrete. It solves the problem that the degree of cement hydration is lowered due to no curing or improper curing, and thus unsatisfactory properties of concrete. 'Internal curing' is allowing for curing 'from the inside to outside' through the internal reservoirs Created. 'Internal curing' is often also referred as 'Self-curing.'

The **ACI-308** Code states that "internal curing refers to the process by which the hydration of cement occurs because of the availability of additional internal water that is not part of the mixing Water."

III. TESTS FOR MATERIALS

Cement is a binder and also a substance that sets and hardens quickly. The cement dries and also reacts with carbon dioxide in the air dependently, and can bind other materials together. Portland cement is by far the most common type of cement in general use around the world. The fineness of cement has an important bearing on the rate of hydration and hence on the rate of gain of strength and also on the rate of evolution of heat. Finer cement offers a greater surface areas for hydration and hence faster the development of strength.

Weigh 100 grams of cement and take it on a standard IS Sieve No. 9 (90 microns). Break down the air set lumps in the sample with fingers. Continuously sieve the sample giving circular and vertical motion for a period of 15 minutes. This weight shall not exceed 10% for ordinary cement.



Figure 3.1 Fineness of Cement

Table 3.1 Test on Material

Sl No	Materials	Test	Result
1	Cement	Fineness	220 m ² /kg
		Initial setting time	120 min
		Final setting time	400 min
		Compressive Strength	43 N/mm ² (OPC 43 grade)
2	C A	Gradation	Zone II
		Specific gravity	2.718
		Water Absorption	0.51 %
3	FA	Gradation	Zone III
		Specific gravity	2.480
		Water Absorption	0.82 %

The standard consistency of cement paste is defined as that consistency which will permit a Vicat plunger having 10mm diameter and 50mm long to penetrate to depth of 33-35 mm from the top of the mould. This apparatus is used to find out the percentage of water required to produce a cement paste of standard consistency. Setting time test has two arbitrary divisions. Vicat apparatus is used to determine the setting of cement.



Figure 3.2 Setting Time Test for Cement

Lower the needle gently and bring it in contact with the surface of the test block and quickly release. Allow it to penetrate into the test block. The period elapsing between the time when water is added to the cement and the time at which needle penetrates is taken as initial setting time. Replace the needle of the Vicat apparatus by a circular attachment. The centre needle makes an impression. The paste has attained such hardness that the center needle does not pierce through the paste more than 0.5mm. The Standard sand is used for finding the strength of cement. Then add water of quantity $p/4 + 3\%$ of combined weight of cement and sand and mix the three ingredients thoroughly until the mixture is of uniform color.



Figure 3.3 Result of Compressive strength

Coarse aggregates are particles greater than 4.75mm are also the raw materials that are an essential ingredient in concrete. Coarse aggregate can also be described as gravel, crushed rock, rocks or stones. Gradation test is mainly done by Sieve analysis. Sieve analysis is conducted to determine the particle size distribution in a sample of aggregates. Grading pattern of a sample of coarse aggregate is assessed by sieving all the samples successively through a set of sieves mounted one over the other in the order of size by keeping the larger sieve on the top. Specific gravity is the ratio of the density of a substance to the density (mass of the same unit volume) of a reference substance. It is determined

by using Pycnometer. The determination of moisture content in the aggregates is mainly to control the quality of concrete particularly with respect to the workability and strength.. In this method drying is carried out in an oven and the loss in weight before and after drying will give the moisture content. Fine aggregates are the aggregate whose size is less than 4.75 mm..The Gradation test of fine aggregate is also the same as that of the coarse aggregate. It is also done by sieve apparatus but the sieves that are arranged vary with that of the coarse

Age (Days)	Compressive strength (N/mm ²)		
	Internally cured concrete		Conventionally cured concrete
	Polyethylene glycol 400 (PEG 400)	Sisal	
3	25.93	27.18	23.30
7	34.66	39.37	38.17
14	41.04	43.41	42.29
28	51.26	53.35	49.00

aggregates.



Figure 3.4 Sieve apparatus

The water absorption of fine aggregate is as same as that of the coarse aggregate and it is done by drying.



Figure 3.5 Pycnometer of sand

IV. MIX DESIGN

The mix design has been carried out for M35 grade of concrete as per the IS10262: 2009. Target mean strength for mix proportioning f_{ck} is 43.25N/mm² for the corresponding Water-Cement ratio of 0.44.

Table 4.1 Mix ratio of materials

Cement (kg/m ³)	FA (kg/m ³)	CA (kg/m ³)	Water (kg/m ³)
340	655.31	1277.7	150
1	1.92	3.75	0.44

The above mix design is derived for the conventional curing process. The polyethylene Glycol 400 and Sisal is added for about 0.5% of weight of cement and the specimens have been casted.

Table 4.2 Compressive strength results

V. CONCLUSION

In this study a comparison is made between the internal cured and conventionally cured concrete. The cubes were casted and the compressive strength was obtained for 3, 7, 14 and 28 days. From these compressive strength results obtained, the internally cured concrete with Sisal fiber have given more compressive strength when compared with the Polymer (Polyethylene Glycol 400). And also the compressive strength of internal curing is higher than that of the conventional curing process.

REFERENCES

- [1] Bentz DP, Lura P, Roberts JW., "Mixture proportioning for internal curing Concrete" Int 2005; 27(2).
- [2] Darryl Anderson, Anderson Engineering and Surveying, Bill DiBrito, DiBrito Material Testing, "Self curing admixture Performance report", February 2012.
- [3] El-Dieb A.S., "Self curing concrete: Water retention, hydration and moisture transport", Construction and building material journal in 2006.
- [4] Hoff, G.C., "Internal Curing of Concrete Using Lightweight Aggregates," Theodore Bremner Symposium, Sixth CANMET/ACI, International Conference on Durability, Thessaloniki, Greece, June 1- 7 (2003).

Modeling and Simulation of Solar PV Cell with MATLAB/Simulink and its Experimental Verification

^[1]K.Mohan, ^[2] Mr.R.Dhinakaran

^[1] PG Student, Department of Mechanical Engineering, Pondicherry Engineering College, pondicherry , India

^[2] Assistant Professor, Department of Mechanical Engineering, Pondicherry Engineering College, Puducherry, India

^[1]kmohan_14@yahoo.com, ^[2]dhinaie@yahoo.com

Abstract— This paper presents the implementation of Solar PV Cell model using MATLAB/Simulink software package. This model is based on mathematical equations. It is described through an equivalent circuit including a photo current source, a diode, a series resistor and a shunt resistor. The proposed model is designed with user-friendly icon and a dialog box like Simulink block libraries. The developed model allows the prediction of Solar PV Cell behavior under given physical and environmental parameters. Taking the effect of sunlight irradiance and cell temperature into consideration, I-V and P-V Characteristics are simulated and compared with experimental results. In order to validate the developed model, an experimental test was conducted and the obtained result produces good agreement with simulation results.

Index Terms— V and P-V Curve, MATLAB/Simulink, Modeling, Simulation, Solar PV Cell.

I. INTRODUCTION

Solar cell is an electrical device that converts energy of light directly into electricity with no pollutant emission. A solar cell is basically a p-n junction fabricated in a thin wafer of semiconductor. The electromagnetic radiation of solar energy can be directly converted to electricity through Photovoltaic effect. When it is exposed to sun light, photons with energy greater than band gap energy of the semi conductor creates some electron-hole pairs proportional to incident irradiation. The renewable energy sources have become more important contributor to the total

energy consumed in the world. In fact, the demand for Solar Energy has increased by 20% to 25% over the past 20 years [1].

The main material used in the photovoltaic industry is Silicon. But there are many lines of research to find materials to replace or supplement Silicon to improve conversion efficiency [2].

There are three major types of PV Cell technology. Those are monocrystalline technology, polycrystalline technology and thin film technology. The monocrystalline and

polycrystalline technologies are based on microelectronic manufacturing technology [1].

I-V curve of Solar PV cell passes through two significant points. (i) Short-circuit current (I_{sc}). It is the current produced when the positive and negative terminals of the cell are short-circuited, and the voltage between the terminals is zero, which corresponds to a load resistance of zero. (ii) Open-circuit voltage (V_{oc}). It is the voltage across the positive and negative terminals under open-circuit conditions, and the current is zero, which corresponds to a load resistance of infinity.

Mathematical modeling of PV Cell is being continuously updated to enable researcher to have better understanding of its working [3].

This paper carried out a MATLAB/Simulink model of polycrystalline solar PV Cell that made possible the prediction of PV Cell behavior under the parameters such as solar irradiance, cell temperature, shunt resistance, series resistance etc.,

II. NOMENCLATURE

V is the output voltage of Solar Cell

I is the output current of Solar Cell

T_{op} is Solar PV Cell operating temperature

T_{ref} is Solar PV Cell reference temperature

I_{ph} Light generated Photo-Current

I_D is the Diode Current of Solar PV Cell

A is an Ideality Factor =1.3 for polycrystalline silicon solar cell

k is Boltzman constant= $1.3805 \times 10^{-23} \text{J/K}$

q is Electron charge= $1.6 \times 10^{-19} \text{C}$

K_i is the Temperature co-efficient of short-circuit current = $0.00017 \text{A/}^\circ\text{C}$

I_{rs} is the cell reverse saturation current(A)

I_{rr} is Operating solar irradiance = 1000W/m^2

I_{sc} is Solar Cell short-circuit current

V_{oc} is Solar Cell open-circuit voltage

N_s is number of cell connected in series

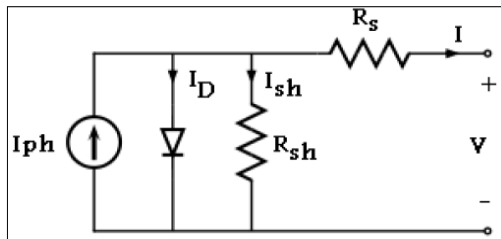
N_p is number of cell connected in parallel

R_s is series resistance of PV cell

R_{sh} is shunt resistance of PV cell

III. MATHEMATICAL MODEL OF SOLAR PV CELL

To understand the Physical behavior of a solar cell, it is useful to create a model which is electrically equivalent, and is based on discrete electrical components whose behavior is well known.



A Solar PV Cell circuit includes current source I_{ph} which represents the cell photocurrent. I_D is Diode current, I_{sh} is the shunt current. R_{sh} and R_s

are the shunt and series resistance of the cell respectively. The equivalent circuit of solar PV cell is shown in Fig.1. Usually the value of R_{sh} is very large and that of R_s is very small, hence they may be neglected to simplify the analysis.[1]. From the equivalent solar PV cell circuit, the current produced by the solar cell is equal to current source (I_{ph}), minus the current flows through the diode (I_D), minus the current flows through the shunt resistor (I_{sh})[2].

The Solar PV cell can be modeled mathematically as given in equations (1)-(5) as per the Theory of semiconductors and Photovoltaics[4] that describes the I-V characteristic of photovoltaic cell.

3.1 Solar cell photo current

The Solar Cell Photo-current (I_{ph}) is depends linearly on solar irradiation (I_{rr}), Short-circuit current (I_{sc}) and also influenced by the temperatures according to following equation.

$$I_{ph} = [I_{sc} + K_i(T_{op} - T_{ref})] * \frac{I_{rr}}{1000} \quad (1)$$

3.2 Solar cell Reverse Saturation current

The Solar Cell Reverse Saturation current (I_{rs}) is depends on Short-circuit current of solar cell, Electron charge, Solar cell operating temperature. It is given by as follows.

$$I_{rs} = I_{sc} / [\exp(\frac{q \cdot V_{oc}}{N_s \cdot A \cdot k \cdot T_{op}}) - 1] \quad (2)$$

3.3 Diode current of Solar cell

Diode current of Solar Cell (I_D) is depends on Reverse saturation of solar cell, Electron charge, Solar cell operating temperature, Boltzman constant, Solar cell Ideality factor etc. It is given by as follows.

$$I_D = I_{rs} * (\exp(\frac{q \cdot (V + I \cdot R_s)}{N_s \cdot A \cdot k \cdot T_{op}}) - 1) \quad (3)$$

3.4 Shunt current of Solar cell

Shunt current of Solar PV cell is varies with Series resistance, shunt resistance, current and voltage across the circuit. It is given as follows.

$$I_{sh} = (V + I \cdot R_s) / R_p \quad (4)$$

3.5 Output current of Solar cell

The Output current of Solar PV cell is given by as follows.

$$I = I_{ph} - I_D - I_{sh} \quad (5)$$

IV. EXPERIMENTAL RESULTS

The solar PV cell used for our study is polycrystalline silicon solar cell having 0.5 volts capacity. It has the dimension of 78mm length and 12mm width. The image of solar cell used for this study is shown in the Fig.2. The Experimental I-V characteristic curve and P-V characteristic curve of solar PV cell measured using Class AAA solar Simulator and its curves are shown in Fig.3 and Fig.4. The experimental results are shown in Table.1.

Solar cell	I_{sc} (A)	V_{oc} (V)	I_m (A)	V_m (V)	P_m (W)	I_{rr} (w/m^2)
Exp	0.35	0.58	0.29	0.44	0.134	1000

I_m is the maximum current, V_m is the maximum voltage, P_m is the maximum power that can be produced by the solar cell.

Fig.2, Image of Solar PV Cell

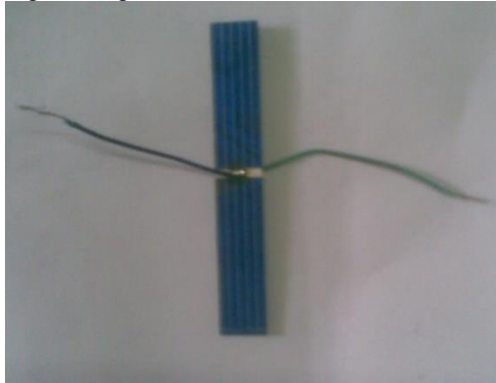


Fig.3, Exp. I-V Curve of Solar PV Cell

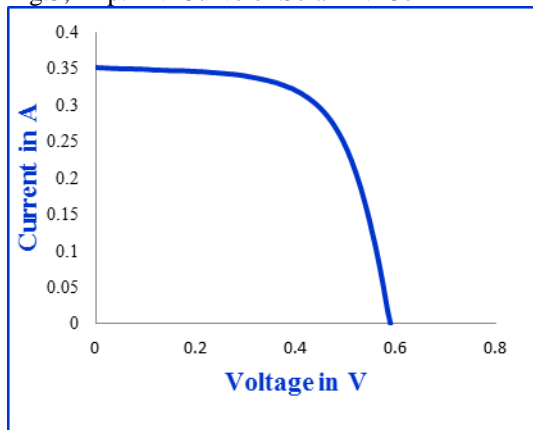


Fig.4, Exp. P-V Curve of Solar PV Cell

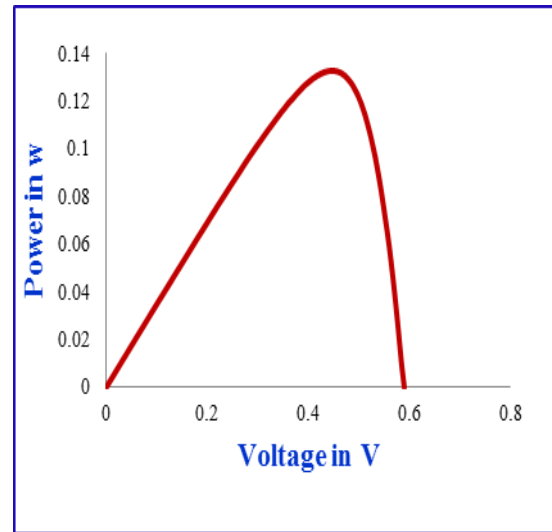


Table 1: Experimental results of solar cell

V. SIMULINK MODEL OF SOLAR PV CELL

Mathematical Modeling of solar PV cell has been done using MATLAB/Simulink. It is based on fundamental circuit equations of solar PV cell as given in the equation from (1)- (5) and also taking account of environmental parameters such as solar irradiance and cell temperature, series resistance, shunt resistance, etc.[3]. The Simulink model of solar PV cell has shown in Fig.5.

VI. SIMULATION RESULTS

Fig.6. shows Simulation result of I-V characteristic curve of solar PV cell obtained from MATLAB/Simulink.

Fig.6, Simulated I-V curve of solar cell

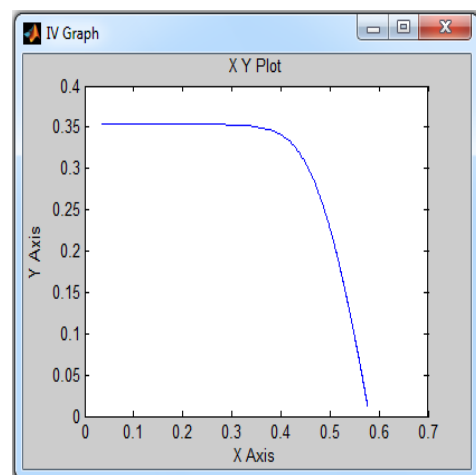
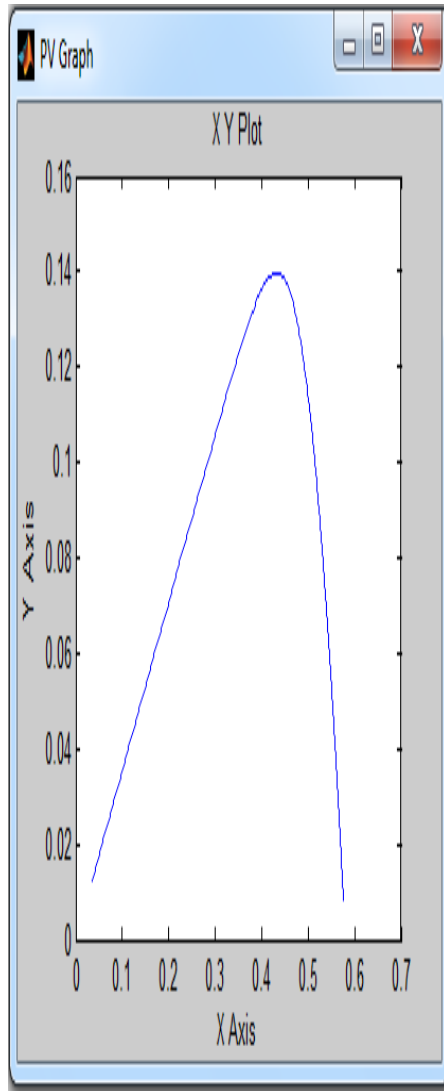


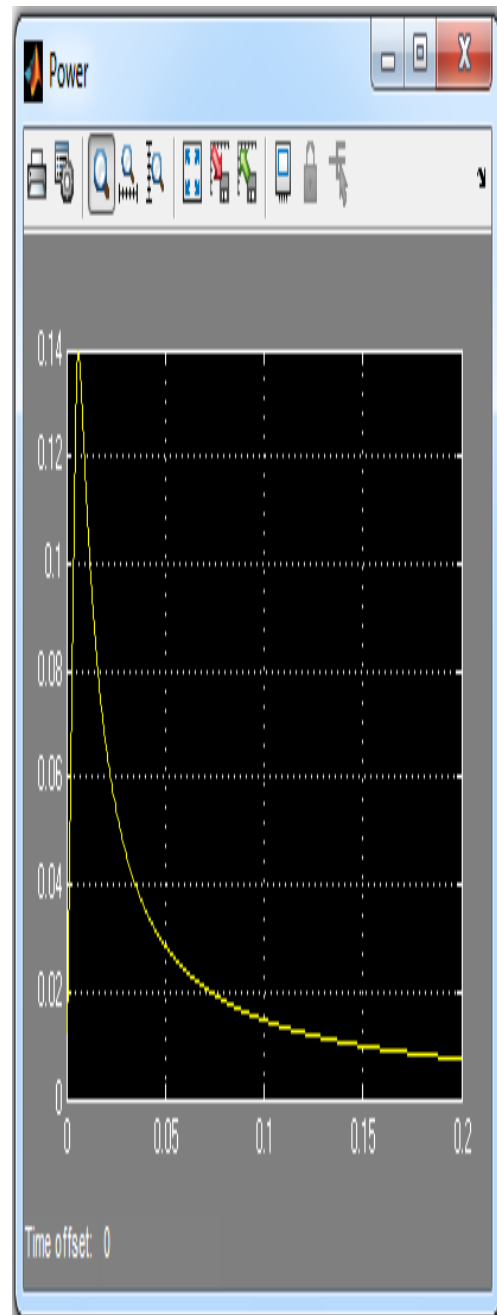
Fig.7. shows simulation result of P-V characteristic curve of solar PV cell obtained from MATLAB/Simulink.

Fig.7, Simulated P-V curve of solar cell



The maximal power that can be produced from the solar cell is about 0.14watts as per the simulation result. Fig.8, confirms maximal power (P_m) value of 0.14 watts from the the solar cell.

Fig.8, Maximim Power point of Solar Cell



From the Get data digitizer software,we are able to track maximum current point (I_m) and maximum voltage point (V_m) based on maximum power point(P_m).

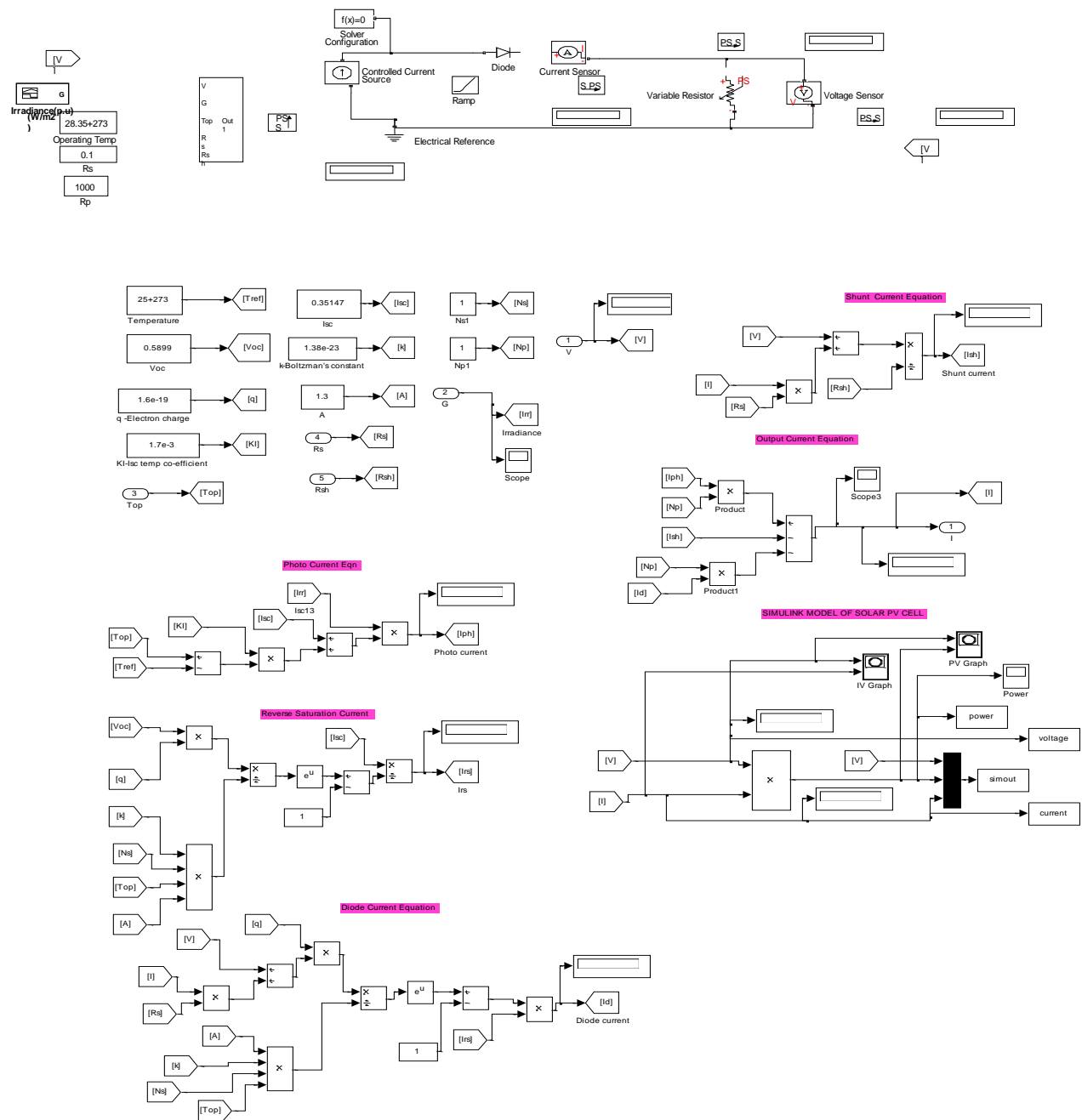


Fig.5. SIMULINK Model of Solar PV Cell

Fig.9, indicates the maximum voltage point from the solar cell is 0.44 volts.

Fig.9, Maximum voltage point of solar cell

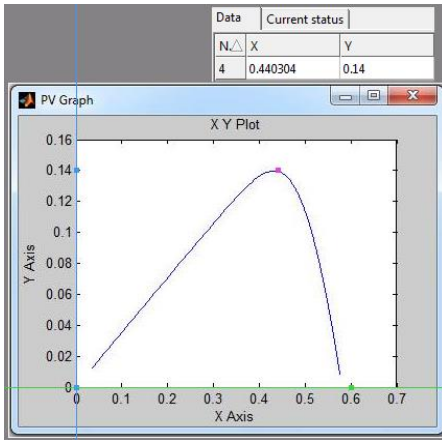


Fig.10, indicates the maximum current point from the solar cell is 0.31 amps. Modeling and experimental results are compared in Table.2.

Fig.10,Maximum current point of solar cell

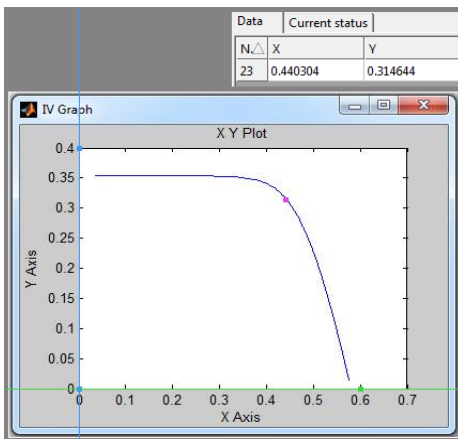


Table 2: Comparison of Experimental & Simulation results of solar cell

Solar cell	I_{sc} (A)	V_{oc} (V)	I_m (A)	V_m (V)	P_m (W)	I_{rr} (w/m^2)
Mod.	0.35	0.58	0.31	0.44	0.14	1000
Exp.	0.35	0.58	0.29	0.44	0.134	1000

VII. CONCLUSION

A Solar PV Cell model based on mathematical model is developed using MATLAB/Simulink and presented in this paper. The model was simulated and validated experimentally using polycrystalline silicon solar PV cell. There is 4.2% error observed from simulation and experimental result at maximum power point of solar PV cell.

Since the field tests can be expensive and depend on weather conditions it is very convenient to have simulation models to enable work at any time. For this reason, In this paper, the development of modeling of solar PV cells has been analyzed.

REFERENCES

- [1] Tarak Salmi, Mounir Bouzguenda, Adel Gastli, Ahmed Masmoudi "MATLAB/Simulink Based Modeling of Solar Photovoltaic Cell" *International Journal of Renewable Energy Research*, Vol. 2, No. 2, 2012
- [2] J.A.Ramos-Hernanz, J.J.Campayo, J.Larranaga, E.Zulueta "Two Photovoltaic Cell Simulation Models In MATLAB/Simulink" *International Journal on Technical and Physical Problems of Engineering*, **4**: 45-51, March 2012
- [3] N.Pandiarajan and Ranganath Muthu "Mathematical Modeling of Photovoltaic Module with Simulink", *International Conference on Electrical Energy Systems*, **3**: 314-319, 2011.
- [4] Aeronautics and Space Administration, (NASA-CR-149364) National, *Solar Cell Array Design Handbook*, vol. 1, Jet Propulsion Lab, 1976.
- [5] Huan-Liang Tsai, Ci-Siang Tu, Yi-Jie Su "Development of Generalized Photovoltaic Model Using MATLAB/SIMULINK" *Proceedings of World Congress on Engineering and Computer Science 2008*, October 22 – 24, 2008, San Francisco, USA
- [6] Jitendra Bikaneria, Surya Prakash Joshi, A.R.Joshi "Modeling and Simulation of PV Cell using One-diode Model" *International Journal of Scientifics and Research Publications*, Vol. 3, Issue 10, October 2013
- [7] S.Rustemli, F.Dincer "Modeling of Photovoltaic Panel and Examining Effects of Temperature in MATLAB/Simulink" *Electronics and Electrical Engineering* Vol No.3, 2011,ISSN 1392-1215.
- [8] Dr. Abu Tariq, Mohammed Asim and Mohd. Tariq "Simulink based modeling, simulation and Performance evaluation of an MPPT for maximum power generation on resistive load" *2nd International Conference on Environmental Science and Technology*, Vol. 6, 2011, Singapore

Technoarete International Conference

Publisher: Technoarete Explore

Website: www.technoarete.com

Supported by:- IFERP-India

www.iferp.in



ISBN

